

1
2
3
4
5
6
7
8
9
10
11
12
13
14
15
16
17
18
19
20
21
22
23
24
25
26
27
28
29
30
31
32

This is a non-peer reviewed pre-print submitted to EarthArXiv.

This manuscript has been submitted to *Journal of Quaternary Science*

Forest or tundra? How different vegetation reconstructions of Last Glacial landscapes in Europe may shape our perception of early human dispersal processes

Oliver A. Kern^{1,2}, Anne Dallmeyer^{1,3}, Andreas Maier⁴, Philipp Schlüter¹, Annika Vogel¹, Nikki Vercauteren¹

¹Institute of Geophysics and Meteorology, University of Cologne, Cologne, Germany

²The Arctic University Museum of Norway, UiT—The Arctic University of Norway, Tromsø, Norway

³Max-Planck-Institute for Meteorology, Hamburg, Germany

⁴Institute for Prehistorical Archaeology, University of Cologne, Cologne, Germany

Contact: oliver.kern@uit.no

Abstract

Regional variability and long-term changes of past ecosystems likely had a strong impact on hunter-gatherer population dynamics, including the expansion of anatomically modern humans and the disappearance of Neanderthals. However, our understanding of these ecosystems remains limited, even when looking at large-scale patterns, such as the extent and distribution of forested areas. Vegetation reconstructions are key to better understand ecological preferences and their influence on the spatial distribution and dispersals of early humans. Here, we compare four different vegetation reconstruction techniques, two based on pollen data and two vegetation models, between 70–20 thousand years before present in Europe. Absolute values in forest cover can differ by up to 40% between reconstruction techniques, highlighting that the choice of method can make the difference between a boreal forest and a tundra. Besides method-specific and statistical uncertainties, the reason for such a substantial offset lies in the loose definition of forest cover metrics, rendering a direct comparison between methods impossible. At the same time, we show that all reconstruction techniques accurately reconstruct ecosystem dynamics over time on continental to regional scales. We therefore highly recommend researchers to use relative forest cover measures as the more robust method to estimate past landscapes.

33 1. Introduction

34 Environmental dynamics are often said to be one of the key aspects in understanding the timing,
35 course, and incentives of the expansion of early modern humans out of Africa and of their dispersal
36 across the world (Maier et al., 2023; Saltré et al., 2024; Timmermann et al., 2022). Yet our
37 comprehension of environmental dynamics during crucial periods of human dispersal remains
38 limited. In particular, it is unclear what role forest cover played during major dispersal events and
39 how different levels of forest cover figured in ecological preference of early hunter-gatherers
40 (Harvati et al., 2019; Hershkovitz et al., 2018). There is growing evidence for an early dispersal of
41 anatomically modern humans into Europe between 55 and 43 ka before present (BP), extending as
42 far west as southern France (Slimak et al., 2022). These presumably very small and rather isolated
43 populations (Mylopotamitaki et al., 2024; Pederzani et al., 2024; Prüfer et al., 2021; Sümer et al.,
44 2025) were contemporaneous to late Neanderthals, who apparently also lived in rather isolated
45 communities (Slimak et al., 2024) and highly structured populations (Rogers, 2024), but disappeared
46 around 43 ka BP from Europe (Posth et al., 2023).

47 To date, there is very little evidence on how the environments that Neanderthals and Palaeolithic
48 hunter-gatherer populations faced may have actually looked like (Fletcher et al., 2010; Tzedakis et
49 al., 2013). Importantly, to assess the possible influence of forestation on habitat fragmentation, the
50 geographic structure of populations, and demographic developments of both Neanderthal and
51 anatomically modern hunter-gatherers, reliable vegetation reconstructions are prerequisite (Maier et
52 al., 2021; Riede and Pedersen, 2018; Schmidt et al., 2021; Staubwasser et al., 2018; Timmermann,
53 2020; Vidal-Cordasco et al., 2023). Such quantitative reconstructions of e.g., forest cover have played
54 a key role in combining archaeological and palaeoenvironmental data on regional scales (e.g., Alenius
55 et al., 2021; Mehl and Hjelle, 2016) and are an important aspect of modern conservation and
56 adaptation strategies (Alkama and Cescatti, 2016; De Lombaerde et al., 2022; Vancutsem et al.,
57 2021). However, previous studies on continental to global scales have either focused on the LGM
58 itself (e.g., Davis et al., 2024; Kaplan et al., 2016) or the period succeeding it (e.g., Li et al., 2025),
59 while palaeoenvironments from the pre-LGM period remain poorly understood.

60 To reconstruct palaeoenvironments, researchers rely on two fundamentally different approaches:
61 Reconstructions based on proxy data and vegetation models. Fossil pollen grains from lake sediments
62 or peat deposits are one of the most common and widespread form of environmental proxy from
63 terrestrial archives. Several different methods, e.g., Biomisation (Prentice et al., 1996), REVEALS
64 (Regional Estimates of Vegetation Abundance from Large Sites; Sugita, 2007), the modern analogue
65 technique (MAT; Zanon et al., 2018), pollen-based temperature reconstructions (Bartlein et al., 2011)
66 transform raw pollen data into reconstructions of environmental and/or climatic conditions.
67 However, predating the Holocene period, suitable pollen archives are scarce and heterogeneously
68 scattered, hampering regional analyses significantly.

69 In contrast, vegetation models offer a continuous reconstruction of palaeoenvironments on global to
70 regional scales (e.g., Beyer et al., 2020; Li et al., 2025) as they operate independently of proxy data
71 and instead use climate variables, such as temperature and precipitation obtained from
72 palaeoclimate simulations. Vegetation models can be implemented in Earth System Models (ESMs),
73 where they are dynamically interacting with the climatic conditions. These so-called dynamic
74 vegetation models (DVMs) are designed to reflect the broad shifts in vegetation patterns and the
75 consequential feedback on the climate system (Dallmeyer et al., 2023). Vegetation models can also
76 operate as static models using the output of palaeoclimate simulations. These models are then used
77 as diagnostic tools based on a pre-defined ruleset. Vegetation models can be implemented at a high
78 spatial resolution to assess specific research questions, such as assessing the local response of
79 ecosystems to (sub)millennial-scale climate variability. Their output is in part validated against

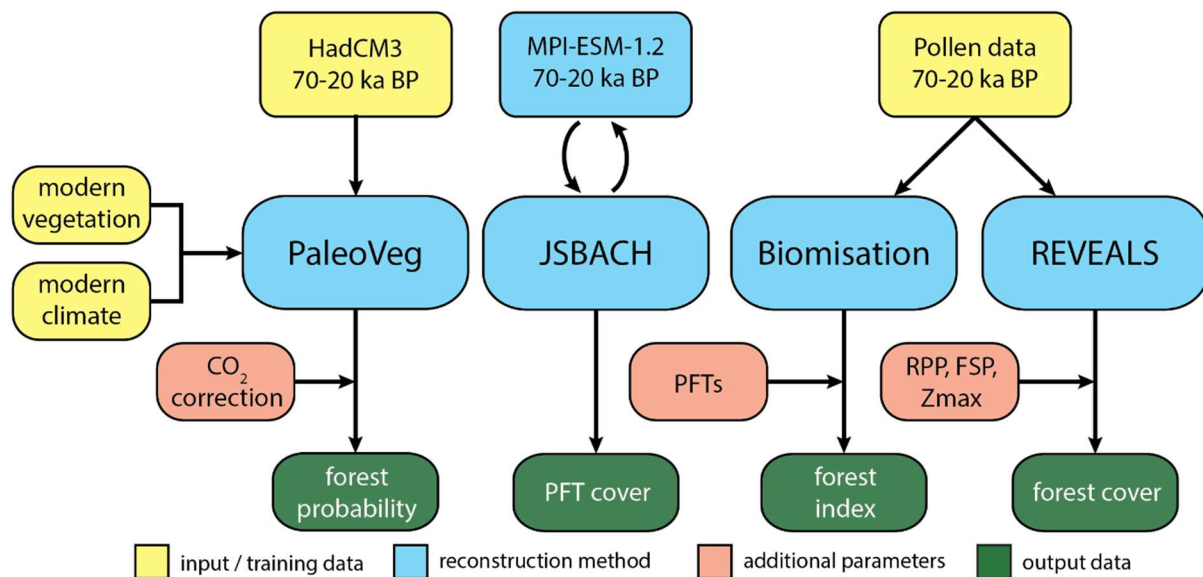
80 modern observations or fossil pollen data (Dallmeyer et al., 2022; Li et al., 2025), but also often
 81 contradicts localised proxy-based reconstructions (Laepfle et al., 2023) thus highlighting important
 82 uncertainties in vegetation reconstructions from both approaches.

83 To obtain as comprehensive an overview as possible of what the landscape may have looked like
 84 during the Late Glacial, we compare the different methods and also address the advantages and
 85 limitations of the available reconstruction approaches. In total, we compare four methods, the
 86 pollen-based Biomisation and REVEALS, a static vegetation model (PaleoVeg), and a DVM (JSBACH)
 87 coupled to an ESM.

88 2. Methods

89 In the following, we briefly describe all methods to reconstruct forest cover during the late Last
 90 Glacial period (70–20 ka BP). For more detailed descriptions, we refer to the references within each
 91 section. Figure 1 presents a schematic overview of the data, methods, and workflow used in this
 92 study.

93



94

95 Figure 1: Schematic overview of the different data and methods used in this study to reconstruct the palaeovegetation.
 96 Input data (yellow) represent the different data sources: The output of high-resolution climate simulations HadCM3 (Beyer
 97 et al., 2020) and MPI-ESM 1.2 (Duque-Villegas et al., 2025), and the compiled fossil pollen data (Kern et al., 2025) for the
 98 period from 70–20 ka BP. Additional parameters (red) originate from other sources (e.g., global CO₂-levels, remote sensing
 99 data, reanalysis data), which are required by the respective methods (blue) to generate different types of vegetation
 100 reconstructions (green). PFT: plant functional type; RPP: relative pollen productivity; FSP: fall speed; Zmax: maximum
 101 spatial extent of the regional vegetation.

102 2.1. PaleoVeg

103 The PaleoVeg vegetation model is extensively described in Shao et al. (2018). The original model used
 104 a probabilistic statistical approach to relate vegetation types to climate variables. In this study, we
 105 utilise a more refined version with a random-forest-based implementation
 106 (<https://github.com/roink/PaleoVeg>; Schlüter, 2025) that is conceptually rooted in Shao et al. (2018)
 107 but not identical to that original setup. PaleoVeg predicts the probability that a certain vegetation
 108 type (including bare soil) exists in each grid cell. The probability that a grid cell is covered by forest
 109 therefore corresponds to the sum of probabilities of all forested vegetation types. Importantly, the
 110 vegetation of a grid cell does not correspond to the vegetation type probabilities (e.g., a grid cell with

111 50 % boreal forest and 50 % tropical forest probabilities is not covered by a mix of boreal and tropical
112 tree taxa).

113 The model statistically reconstructs the palaeovegetation by applying a present-day vegetation-
114 climate relationship to climatic states of the past. It was trained using remote sensing data with a
115 spatial resolution of 8 km from the Advanced Very High Resolution Radiometer (AVHRR, Loveland et
116 al., 2000) and the WorldClim 2.1 data based on 1970–2000 climate (Fick and Hijmans, 2017). The
117 approach has been validated by reconstructing the modern vegetation using the WorldClim data and
118 comparing it to the original AVHRR vegetation dataset (Shao et al., 2018). The model then applies the
119 same relationship to past climate states in order to statistically reconstruct the palaeovegetation
120 following a modified classification by the International Geosphere-Biosphere Programme (Loveland
121 et al., 2000) adapted to the pre-Holocene period (e.g., removal of “urban land” and “cropland”). The
122 final classification consists of 10 vegetation types and bare ground. As input data, we use the
123 downscaled and bias-corrected palaeoclimate data based on the HadCM3 global climate model
124 (GCM; Beyer et al., 2020). The HadCM3 dataset comprises 17 bioclimatic variables (BCVs) for 120–
125 0 ka BP in 1,000-year (22–0 ka BP) and 2,000-year (120–22 ka BP) time steps at a spatial resolution of
126 0.5° and is accessible through the *pastclim* R package (Leonardi et al., 2023).

127 Atmospheric CO₂ considerably influenced photosynthesis efficiency in past ecosystems (Prentice and
128 Harrison, 2009). The PaleoVeg thus also factors in a CO₂ correction factor (f_{CO_2}) that was initially
129 inferred from palaeovegetation reconstructions for the LGM (Willez et al., 2011). Assuming a linear
130 relationship between CO₂ levels and photosynthesis rates (where $f_{CO_2} = 1$ for the present), we
131 extrapolated f_{CO_2} for the entire study interval (see Supporting Information) using atmospheric CO₂
132 data from Antarctic ice cores (Indermühle et al., 2000; Veres et al., 2013).

133 **2.2. MPI-ESM-1.2 and its land component JSBACH**

134 We use the vegetation output of a transient simulation (Duque-Villegas et al. 2025) performed in the
135 comprehensive Earth System Model MPI-ESM-1.2 (Max-Planck-Institute Earth System model version
136 1.2, Mauritsen et al., 2019). This simulation covers the entire Last Glacial, but we concentrate on the
137 period from 70 to 20 ka BP. The MPI-ESM 1.2 includes the land surface and dynamic vegetation
138 model JSBACH3.2 (Reick et al., 2013) that represents vegetation in the form of eight plant functional
139 types (PFTs) as a fraction of land-cover in any given grid cell. These include extratropical and tropical
140 trees that can either be deciduous or evergreen, raingreen and cold-resistant shrubs, and C3 and C4
141 grasses. JSBACH uses a “mosaic” approach, where each land surface grid cell is tiled so that all PFTs
142 could in principle coexist within a grid cell. The PFTs are limited by temperature thresholds reflecting
143 their bioclimatic tolerance (e.g., cold resistance, chilling, and heat requirements). Shifts in PFT cover
144 are driven by the relative differences in net primary productivity (NPP) between the PFTs, which
145 depend on factors such as moisture availability or atmospheric CO₂-levels, and reflect inter-PFT
146 competition (Brovkin et al., 2009). The JSBACH version used in this simulation does not include
147 permafrost, dynamic soil development, or seed dispersal. Thus, timescales of vegetation migration
148 are relatively short compared to reality (Dallmeyer et al., 2022). The spatial resolution of the
149 simulation is T31, i.e. 400 km x 400 km grid-cell size on a Gaussian grid.

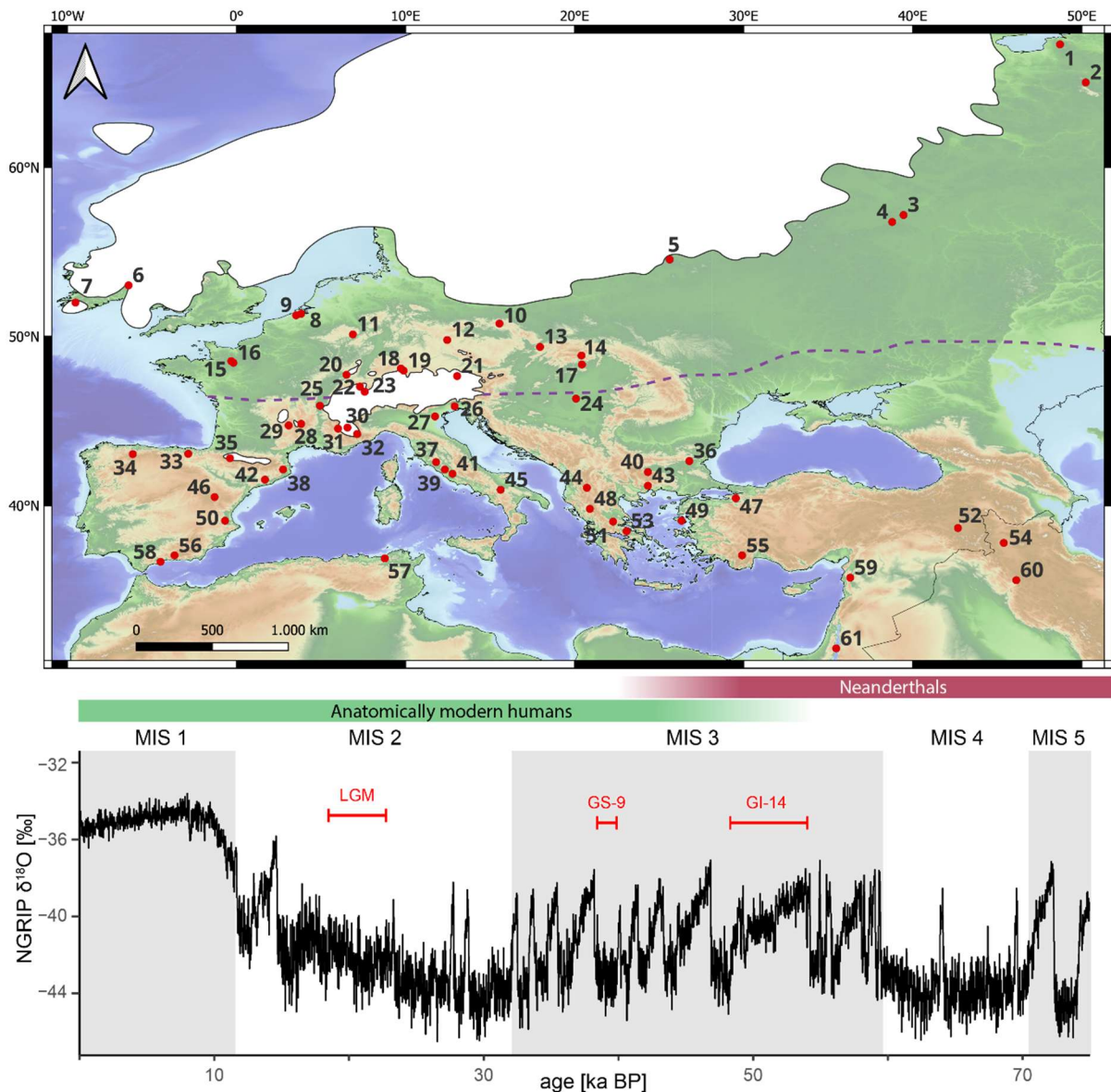
150 **2.3. Pollen data**

151 We compiled 61 palynological records from palaeoclimate archives located in Europe and the
152 surrounding areas (Fig. 2) that contain pollen data from the late Last Glacial period, specifically the
153 interval from 70–20 ka BP (Kern et al., 2025). Pollen samples were selected within ± 500 years of the
154 defined time step (e.g., 30,000 ± 500 years BP). If multiple data points fall into this window, pollen
155 counts were aggregated into a single sample. Prior to data analyses, all taxa were harmonised to the

156 genus (woody and major herbaceous taxa) or the family level (other herbaceous taxa) (Kern et al.,
157 2025). This fossil pollen dataset forms the basis for the Biomisation and REVEALS reconstructions
158 (Fig. 1). It is important to note that both pollen-based methods can only represent the vegetated
159 area (since pollen data are unable to represent bare soil).

160 The Biomisation process describes the grouping of plant taxa into plant functional types (PFTs) based
161 on their climatic preferences and similar traits (e.g., life form, leaf morphology, and phenology). Sets
162 of PFTs are then arranged in combinations to form a relatively small number of biomes, i.e., a
163 biological community that formed as a result of environmental and climatic factors. The Biomisation
164 algorithm (Prentice et al., 1996) utilises PFTs of the total pollen sum to calculate the most probable
165 biome. This relatively simple reconstruction algorithm has been shown to perform moderately well
166 and addresses differences in pollen productivities between tree/shrub and forb taxa (Binney et al.,
167 2017). In this study, we use 30 PFTs to reconstruct 12 biomes after Bigelow et al. (2003) and Binney
168 et al. (2017). The Biomisation algorithm yields so-called biome affinity scores, dimensionless scores
169 that measure the similarity of the record to a predefined set of biomes (Prentice et al., 1996). The
170 biome with the highest affinity score is then assigned to a site. We here introduce a quantitative
171 measure (forest index) to estimate the probability that a site is covered by a forested biome. This is
172 calculated as the maximum affinity score within all forested biomes (e.g., cool mixed forest) minus
173 the maximum affinity score within all non-forested biomes (e.g., cushion-forb tundra), which is then
174 rescaled to 0-100.

175 The REVEALS algorithm reconstructs land-cover estimates (Sugita, 2007) and has been described and
176 discussed extensively in previous studies (Githumbi et al., 2022; Kern et al., 2025; Pearce et al., 2023;
177 Serge et al., 2023). REVEALS yields land-cover percentages for every taxon (Sugita, 2007); tree cover
178 can then be calculated as the sum of land-cover by all tree taxa. The unique feature of REVEALS is the
179 addition of taxa-specific parameters, such as the relative pollen productivity (RPP) estimates and the
180 fall speed of pollen (FSP), to the raw pollen counts. Multiple compilations of RPP and FSP values on
181 regional to continental scales exist (e.g., Githumbi et al., 2022; Schild et al., 2025; Serge et al., 2023;
182 Wiczorek and Herzschuh, 2020) and have been validated and optimised through comparison with
183 satellite-based land-cover reconstructions (Hansen et al., 2013; Schild et al., 2025). Lastly, REVEALS
184 accounts for wind speed, and the maximum extent of regional vegetation (Z_{max}), which were set to
185 3 m/s and 100 km, respectively (Trondman et al., 2015). REVEALS provides land-cover percentages
186 for each taxon, which can be assigned to e.g., biomes based on the individual research questions
187 (e.g., Githumbi et al., 2022; Kern et al., 2025).



188

189 Figure 2: Pollen archives included in this study (after Kern et al., 2025) next to NGRIP $\delta^{18}\text{O}$ for the last 75 ka (Rasmussen et al., 2014). The extent of ice-sheets (Ehlers et al., 2011) and permafrost (Stevens et al., 2025) is shown for the Last Glacial
 191 Maximum. The three red intervals (LGM, GS-8, and GI-14) are referred to in the results and discussion section. Coloured
 192 bars indicate the estimated presence of different human species in Europe (after Slimak et al., 2022). Marine Isotope Stages
 193 (MIS) after Lisiecki and Raymo (2005).

194 **2.4. Definition of forest cover**

195 Forest cover is often interpreted as the density and extent of tree cover and has been extensively
 196 used in palaeoecological studies (Pearce et al., 2023; Zanon et al., 2018) and climate-vegetation
 197 feedback studies on albedo or evapotranspiration, where forest cover is often more relevant than
 198 the vegetation composition (Bright et al., 2015; Reichstein and Carvalhais, 2019). However, the term
 199 “forest cover”, albeit widely used, is only loosely defined. Forest cover can mean that the dominant
 200 biome is a type of forest, that the probability of a forested biome domination is higher than a
 201 threshold (e.g., 50 %), or that the sum of forest biome probabilities is higher than a threshold.
 202 Furthermore, it is often incorrectly associated with the term “tree cover”, although a forest is very
 203 rarely composed only of trees (in terms of land cover, i.e., a fully closed canopy).

204 Palaeovegetation reconstructions can be used to reconstruct forest cover, but they typically vary in
 205 their respective outputs, including categorical (e.g., presence/absence, biomes), semiquantitative

206 (e.g., biome affinity scores, a dimensionless score to determine the most plausible biome), and
207 quantitative data (e.g., biome percentages, taxon percentages, tree cover fractions). Additionally,
208 methods can treat unvegetated areas (e.g., bare soil) differently in their calculations (e.g., Dallmeyer
209 et al., 2025; Li et al., 2025; Strandberg et al., 2022; Sun et al., 2022). As a consequence, the respective
210 absolute values of forest index (Biomisation), forest cover (REVEALS), tree cover fraction (JSBACH),
211 and forest probability (PaleoVeg) must be interpreted differently.

212 A direct comparison of such techniques has been successfully implemented in various studies,
213 covering a wide range of temporal and spatial scales (Dallmeyer et al., 2023; Hallett et al., 2025;
214 Pearce et al., 2025; Schild et al., 2025; Zanon et al., 2018). However, this requires the introduction of
215 a universal biome definition scheme across methods (Dallmeyer et al., 2019). This becomes
216 increasingly difficult when more than two methods are compared and often entails a loss of
217 information from oversimplification. In this study, we therefore decided to evaluate and compare the
218 different representations of forest cover for each respective vegetation reconstruction technique,
219 without trying to shoehorn them into an overarching scheme. As a consequence, absolute values of
220 forest cover should be interpreted with caution. Instead, we focus on temporal trends, amplitudes of
221 change, and regional patterns in the vegetation. To facilitate the direct comparison between
222 methods, we standardise all datasets by subtracting the respective mean and dividing by the
223 standard deviation. The resulting values (also known as Z-scores) have a mean of 0, with positive
224 values indicating above average forest cover and vice versa.

225 **2.5. Chronological uncertainty**

226 Chronological uncertainties are typically reported in studies as errors in direct dating techniques
227 (e.g., radiocarbon dating or luminescence dating) or as model uncertainties. However, most of the
228 time, chronological uncertainties are difficult to quantify as they result from a complex interplay of
229 multiple factors that contribute differently at any given time in a time series. These factors include,
230 but are not limited to, dating uncertainty, interpolation between absolute dates, uncertainties
231 resulting from correlation techniques, sampling uncertainties, temporal binning of data, and phase
232 shifts.

233 To investigate the level of chronological uncertainty and to avoid misinterpretation of datasets, we
234 employed two methods to quantify whether chronological uncertainties substantially contribute to
235 potential agreements or mismatches between reconstruction techniques: Time-lagging and dynamic
236 time warping (DTW). Time-lagging describes the temporal shift of one dataset by one or more time
237 steps in either direction. Subsequent analyses such as the Root Mean Square Deviation can then
238 identify whether the time-lagged data are a better fit than the original, which might indicate a
239 systematic temporal offset.

240 DTW works similar to time-lagging, but on a point-by-point basis. It computes the local stretch or
241 compression applied to two timeseries in order to minimise the observed distance between both
242 (Giorgino, 2009). The DTW distance then yields information on the similarity between two time
243 series after alignment and thus corrects for potential chronological uncertainties. Furthermore, we
244 compare the Root Mean Square Deviation before and after DTW was applied for each method pair.
245 DTW was performed on standardised Z-scores in R using the package *dtw* and employing the
246 Rabiner-Juang step pattern type "VI-c" (Giorgino, 2009).

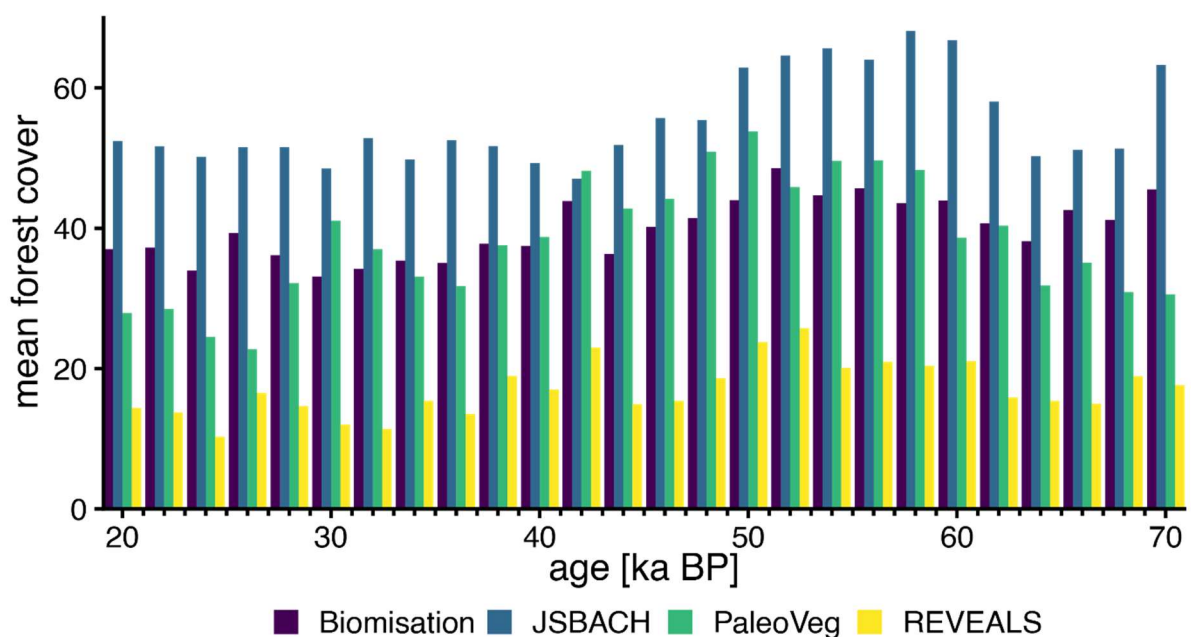
247 3. Results

248 3.1. Temporal evolution of mean forest cover

249 We employed forest-cover reconstructions for all methods from 70 ka BP to 20 ka BP in time steps of
250 2000 years (i.e., 26 time steps). For this calculation, we consider only grid cells (PaleoVeg and
251 JSBACH) where pollen data are available for the same time step. Overall, JSBACH consistently
252 reconstructed the highest (mean 55 %) and REVEALS the lowest (mean 17 %) levels of forest cover
253 across all time steps. Biomisation (mean 40 %) and PaleoVeg (mean 38 %) range in-between (Fig. 3).
254 Importantly, we observe a clear offset between methods across all time steps. Compared to
255 PaleoVeg and the Biomisation values, the forest reconstructions of JSBACH and REVEALS consistently
256 range higher and lower, respectively. Based on the definition of forest cover and the differences in
257 the calculation of forest cover from the individual method outputs (as discussed in section 2.4), this
258 behaviour was expected and hinders a direct comparison between methods, because the absolute
259 values are not comparable.

260 To circumvent this general offset in forest cover reconstruction, each method was normalized by
261 calculating their respective Z-scores. The resulting data from of all methods highlight several
262 important features (Fig. 4): The overall patterns of reconstructed forest cover are in agreement
263 across all methods and broadly represent the climatic conditions during the Last Glacial period.
264 Lower forest values from 70–60 ka BP broadly correspond to MIS 4, although the different methods
265 show some disagreement on the exact timing of the MIS 5a–MIS 4 transition. An abrupt increase in
266 forest values across all methods signals the transition into MIS 3, with the highest values between
267 60–50 ka BP and a gradual decrease to lower values until ca. 30 ka BP. Within this gradual decrease,
268 several smaller increases in values can be observed that may correspond to interstadials, but these
269 are not consistent across methods. The absence of individual interstadials is likely due to the binning
270 of data into relatively broad bins of 2 kyr, which is longer than most interstadials during MIS 3. The
271 transition into early MIS 2 and the LGM is hardly discernible from the data.

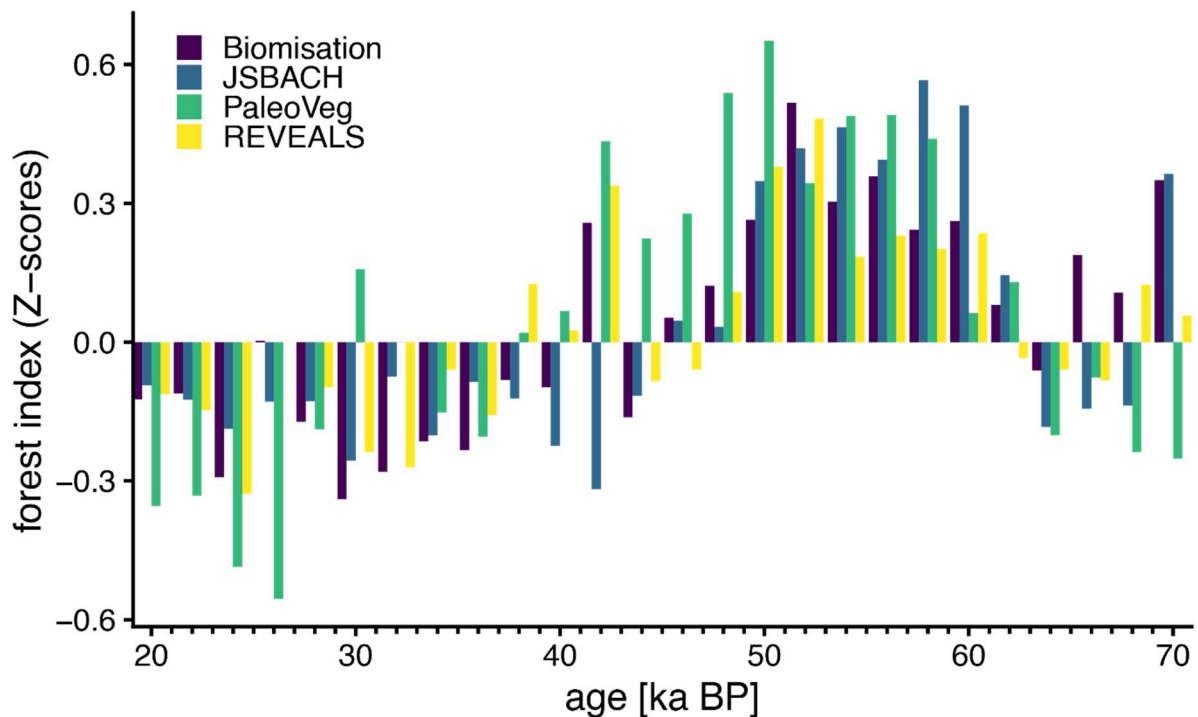
272



273

274 Figure 3: Comparison of the mean forest cover generated by each method in Europe during the 70–20 ka BP interval. The
275 respective means for PaleoVeg and JSBACH were only calculated across grid cells where pollen data was available at a given
276 time step. Absolute values can differ by up to 40 % (JSBACH and REVEALS) resulting from the different definitions of forest

277 cover (see section 2.4), but the overarching temporal pattern is shared across all datasets and broadly follows the climate
278 signal observed in the Northern Hemisphere (Fig. 2, Rasmussen et al., 2014).



279

280 Figure 4: Temporal evolution of forest reconstructions from 70–20 ka BP in Europe after Z-score normalisation.
281 Standardisation removes the general offset between datasets (Fig. 3) and highlights that all methods share a similar
282 temporal trend.

283 3.2. Time-lagging and dynamic time warping

284 To evaluate a potential chronological offset between datasets, we calculated the correlation
285 coefficients (R) between method pairs after shifting one dataset by one time step in either direction
286 (i.e., ± 2000 years). In the majority of cases, correlation decreased substantially after time-lagging.
287 Two exceptions include the Biomisation-JSBACH and PaleoVeg-JSBACH pairs, where the R values
288 improved marginally from 0.589 to 0.595 and 0.808 to 0.818, respectively. However, lagging the
289 JSBACH dataset by one time step also reduces the correlation between the REVEALS-JSBACH pair
290 substantially (from 0.704 to 0.606). Hence, we chose not to systematically lag any dataset for future
291 analyses.

292 Instead, we investigated how well-aligned individual datapoints are across all datasets. For this, we
293 performed pairwise DTW on the mean forest cover percentages across the entire domain for every
294 time step (Giorgino, 2009). DTW calculates the cost of the optimal warping path (DTW distance; low
295 distances indicate a higher similarity). Here, we chose the step pattern “Rabiner-Juang type VI-c”,
296 which resulted in a minor time-series alignment at the cost of warping the time series to an extent.
297 The observed DTW distances (Tab. 2) after alignment range from 0.60 to 0.86 indicating a weak to
298 moderate similarity. Overall, the improvements in the correlation coefficient before and after
299 alignment were minor; the only exception being the JSBACH-Biomisation pair, where the correlation
300 coefficient after alignment improved by 0.22.

301 In summary, both time-lagging and DTW revealed no systematic offset between datasets. Minor
302 improvements can be achieved by DTW for specific data-pairs, but this would also negatively affect
303 the correlation between other pairs. Hence, we refrain from aligning datasets only to improve the
304 correlation of specific method-pairs.

305 Table 1: Correlation coefficient (R) of the warped mean forest cover time series after dynamic time warping (R before time-
 306 warping in parentheses). The REVEALS-Biomisation pair is omitted from the analysis, because both methods originate from
 307 the same pollen dataset.

	REVEALS	JSBACH	Biomisation	PaleoVeg
PaleoVeg	0.74 (0.65)	0.86 (0.81)	0.60 (0.54)	-
JSBACH	0.76 (0.70)	-	0.81 (0.59)	0.86 (0.81)

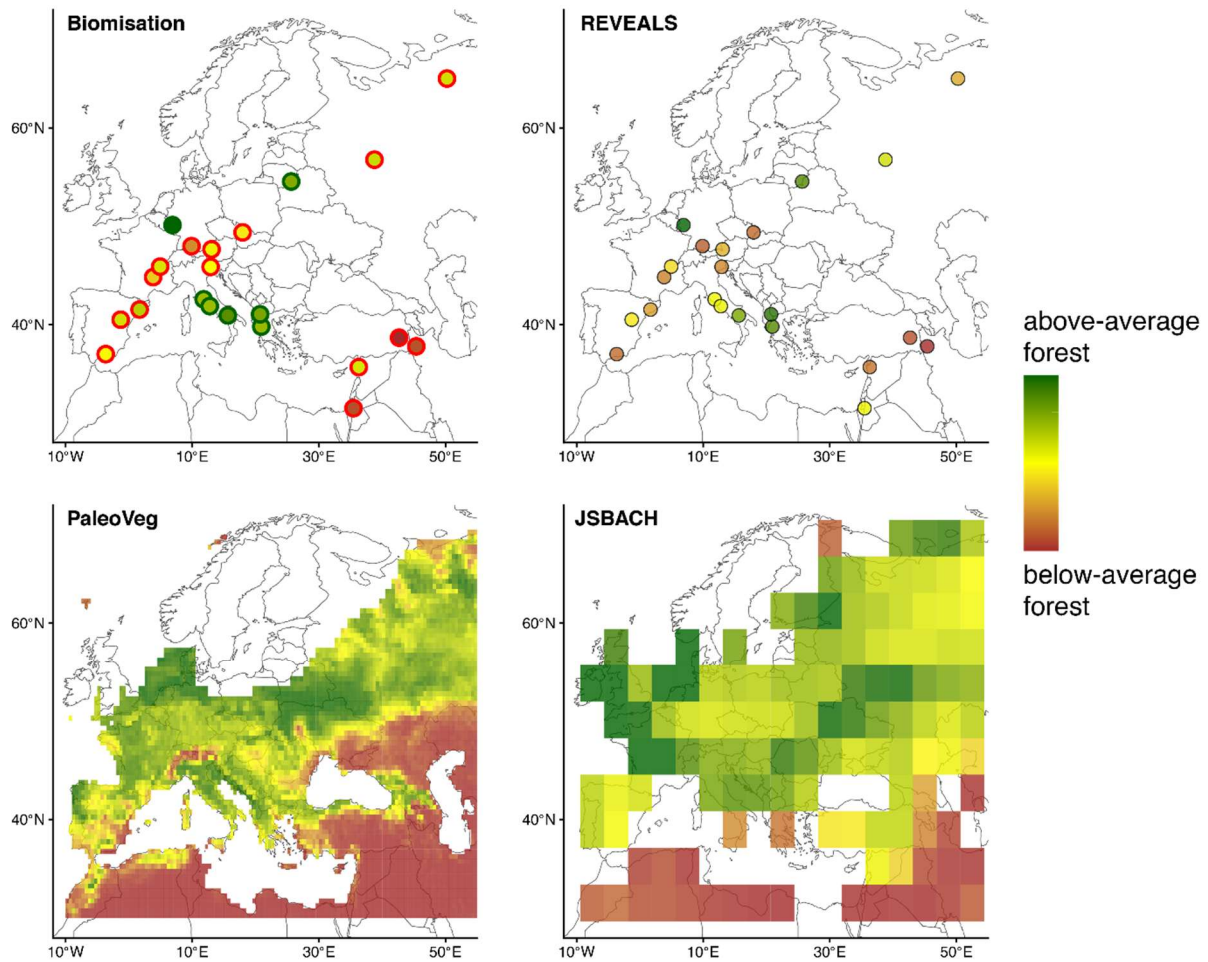
308

309 3.3. Spatio-temporal distribution of forest cover

310 In the following, we briefly present changes in forest-cover reconstructions for each method at three
 311 selected time intervals: Greenland Interstadial 14 (GI-14; ca. 52 ka BP), Greenland Stadial 8 (GS-8, ca.
 312 36 ka BP) and the Last Glacial Maximum (LGM, ca. 22 ka BP). These snapshots represent interstadial,
 313 stadial, and full glacial conditions during MIS 2–3, respectively. Importantly, the timing of stadials and
 314 interstadials is well-aligned between the NGRIP $\delta^{18}\text{O}$ climate reference dataset (Rasmussen et al.,
 315 2014), the MPI-ESM simulation (including JSBACH) (Duque-Villegas et al., 2025), and the HadCM3
 316 output (used for PaleoVeg; Beyer et al., 2020). Forest-cover reconstructions are presented as
 317 standardised Z-scores, i.e., as deviations from the mean forest cover of the respective method, to
 318 compensate for the systematic offset between methods (Figs. 3 and 4).

319 3.3.1. Forest cover during GI-14 (interstadial conditions)

320 The forest cover in Europe during GI-14 (52 ka BP; Fig. 5) represent the maximum forest cover in the
 321 investigated time frame (70–20 ka BP). High levels of forest cover are observed north of the Alps and
 322 in the Central Mediterranean region, while Northern Africa and the Middle East remained mostly
 323 treeless and the Western and Eastern Mediterranean (the Iberian Peninsula and Anatolia) are
 324 characterised by lower forest cover compared to the rest of Europe. All methods agree that the
 325 northernmost ice-free regions of Central Europe were likely forested, but the individual amount (with
 326 respect to their means) can vary substantially. In contrast, the Alpine region shows lower forest cover
 327 in all methods except JSBACH.

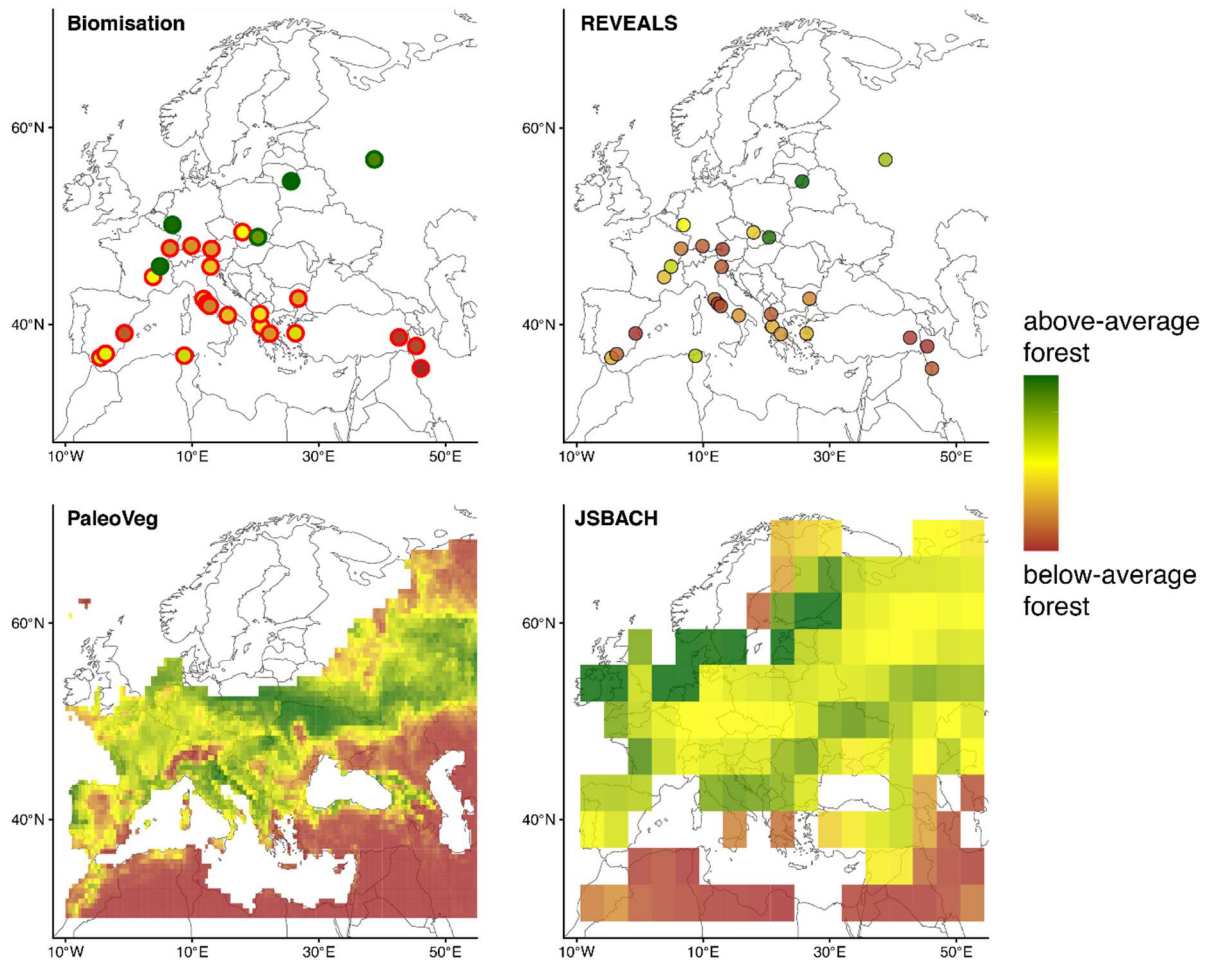


328

329 Figure 5: Forest cover Z-scores (with respect to the 70–20 ka BP interval) for all different methods in Europe during
 330 Greenland Interstadial 14 (GI-14; 52 ka BP). Green values depict a above-average forest cover, while red values show
 331 below-average forest cover. For Biomisation, the borders of each site indicate whether the Biomisation predicted a forest
 332 biome (green) or a non-forest biome (red).

333 3.3.2. Forest cover during GS-8 (stadial conditions)

334 Compared to GI-14, the mean forest cover during GS-8 (36 ka BP; Fig. 6) are considerably lower and
 335 closer to the respective means for the entire study interval (i.e., yellow in Fig. 6). The overall pattern
 336 of forests across Europe remains similar to that of GI-14, but with a stronger North-South divide.
 337 Regions of high forest cover stretch across Central and Eastern Europe in an E-W belt, while forest
 338 cover levels, especially in the pollen-based methods, have decreased substantially south of the Alps.
 339 Particular the Italian Peninsula and the Balkans show lower forest cover compared to GI-14. The
 340 remainder of the Mediterranean and the Middle East remain unchanged. The site in Tunisia
 341 highlights that while the majority of Northern Africa is virtually treeless, small islands of forests can
 342 persist if the local conditions are favourable.



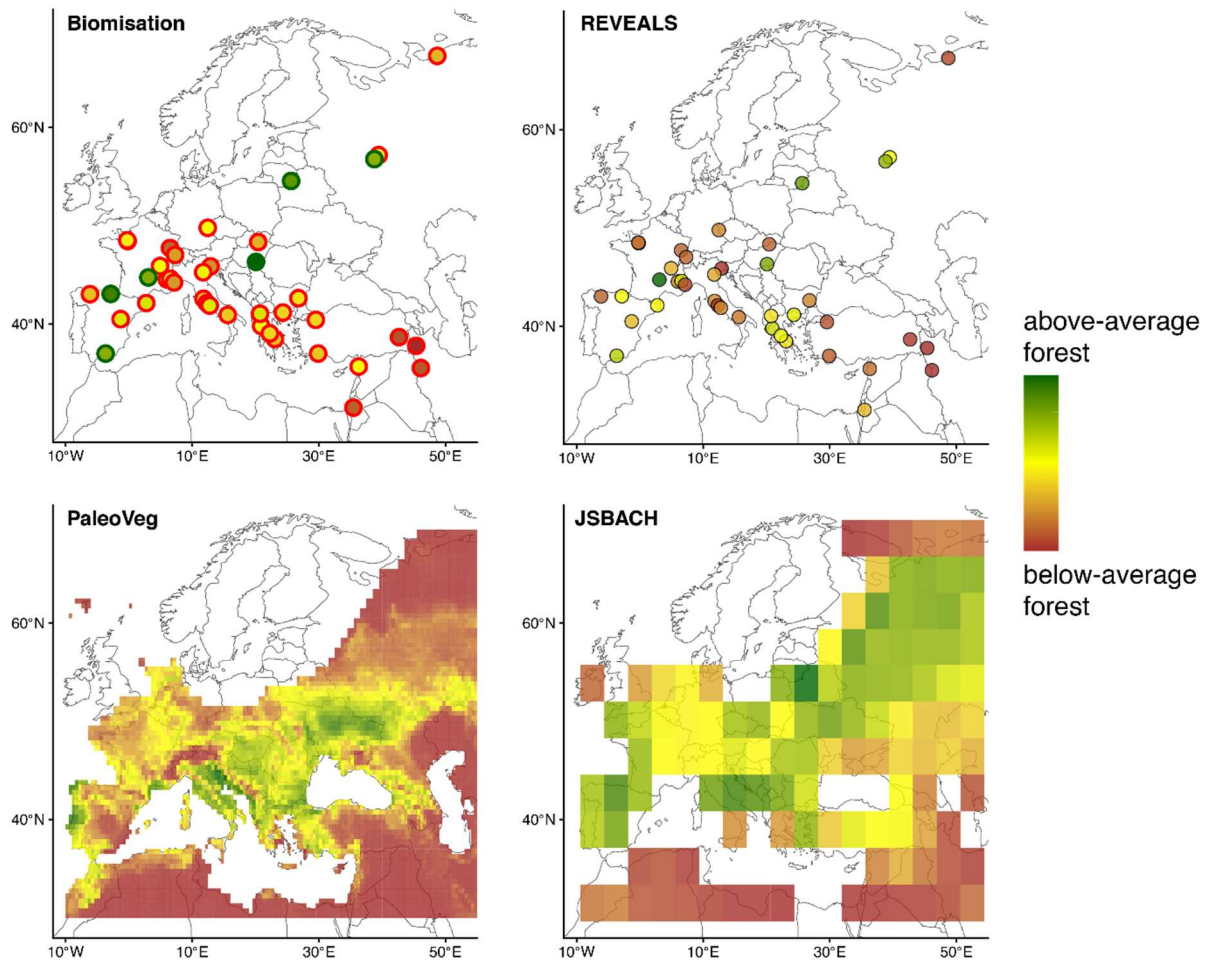
343

344 Figure 6: Forest cover Z-scores (with respect to the 70–20 ka BP interval) for all different methods in Europe during
 345 Greenland Stadial 8 (GS-8; 36 ka BP). Green values depict a above-average forest cover, while red values show below-
 346 average forest cover. For Biomisation, the borders of each site indicate whether the Biomisation predicted a forest biome
 347 (green) or a non-forest biome (red).

348 3.3.3. Forest cover during the LGM (full glacial conditions)

349 During the full glacial conditions of the LGM (22 ka BP; Fig. 7) levels of forest cover are close to their
 350 minima. Nonetheless, isolated regions with above-average forest cover remain throughout Europe,
 351 but primarily in coastal regions of Southern Europe (Iberian Peninsula and Adriatic coast) and Eastern
 352 Europe (Pannonian Basin and the East European Plain). In contrast, the levels of forest cover have
 353 decreased substantially from GS-8 and GI-14 in North-Eastern Russia, Central and Western Europe.
 354 No methods predict a significant presence of forests in Northern Africa and the Middle East.

355



356

357 Figure 7: Forest cover Z-scores (with respect to the 70–20 ka BP interval) for all different methods in Europe during the Last
 358 Glacial Maximum (LGM; 22 ka BP). Green values depict a above-average forest cover, while red values show below-average
 359 forest cover. For Biomisation, the borders of each site indicate whether the Biomisation predicted a forest biome (green) or
 360 a non-forest biome (red).

361 4. Discussion

362 Environmental change in Europe during the Last Glacial was naturally tied to the long- and short-
 363 term climatic evolution. Over longer timescales of several millennia, terrestrial ecosystems in Europe
 364 are broadly in tune with the climatic patterns observed in Greenland ice cores (Rasmussen et al.,
 365 2014). The fully glacial climates of MIS 4 and MIS 2 led to cold and dry conditions across Europe,
 366 which substantially limited the proliferation and spread of tree taxa (e.g., Fletcher et al., 2010; Kaplan
 367 et al., 2016). During MIS 3, more mild and humid climatic conditions favoured an increase in forest
 368 cover and the expansion of tree species into the higher latitudes. This was particularly pronounced
 369 during interstadials – transient bursts of warming and increased moisture availability – which led to a
 370 rapid afforestation across wide areas of Europe (Allen et al., 2000; Britzius et al., 2024; Kern et al.,
 371 2022). Although the return to stadial conditions entailed forest contractions, the overall levels of
 372 forest cover during MIS 3 remained well above those during the full glacial conditions of MIS 4 and
 373 MIS 2.

374 This overarching pattern of climate-ecosystem coupling is well-represented in all methods
 375 investigated in this study (Figs. 3 and 4). On continental scales, the resulting reconstructions show a
 376 moderate to high correlation with each other. However, on local scales, the reconstruction of forest
 377 at a specific site and the associated grid-cell may vary substantially. To an extent, this is to be
 378 expected and stems from of a combination of factors such as statistical variance, chronological

379 uncertainty, and model and proxy data (in-)accuracy. In the following, we explore in more detail the
380 regional patterns of forest cover in Europe during the Last Glacial, how the different methods
381 perform, as well as their strengths and weaknesses.

382 **4.1. Regional forest cover**

383 The reconstructions of regional forest cover exhibit a wide range of potential palaeoenvironments in
384 Europe during the Last Glacial (Fig. 5–7). Regions at lower latitudes, such as Northern Africa and the
385 Middle East, experience little variability in forest cover throughout the entire time interval. To some
386 extent, the reconstructions in these regions even suggest a slight afforestation during cold intervals
387 such as the LGM compared to the preceding MIS 3. This is likely related to the southward shift of
388 moisture belts, increasing overall precipitation and decreasing precipitation seasonality in proxy-
389 based and model-based climate reconstructions (Arpe et al., 2011; Davis et al., 2024; Ludwig et al.,
390 2016). Despite the cooler LGM temperatures and lower CO₂ levels stunting tree growth (Wolfe et
391 al., 2011), higher moisture availability outweighs these factors at lower latitudes to an extent.

392 In the Mediterranean, the vegetation response pattern to climatic variability is highly differentiated.
393 While much of the Mediterranean region exhibits a moderate decrease in forest cover from
394 interstadial to stadial as well as stadial to full glacial climates (Figs. 5–7), smaller sub-regions diverge
395 from the overall pattern. For example, the north-western Iberian Peninsula, the Balkans, and Central
396 Italy exhibit a certain resilience to climatic perturbations. Model data show that these areas retained
397 a high forest cover during e.g., the LGM, indicating that these areas may have acted as glacial refugia
398 during the Last Glacial. Unfortunately, these model predictions cannot be validated due to the
399 limited number of pollen-based reconstructions (Fig. 2; c.f. Fletcher et al., 2010) and plant
400 macrofossil data (e.g., Tzedakis et al., 2013) in these critical areas.

401 Changes in forest cover in response to climatic perturbations are relatively homogeneous in Western
402 and Central Europe. Interstadial conditions favoured the widespread expansion of trees and resulted
403 in vast regions of high forest cover (Fig. 5). During stadial conditions, intermediate levels of forest
404 cover reflect transitional ecological conditions (Fig. 6). Full glacial conditions are dominated by open
405 landscapes, albeit the datasets hint at the persistence of isolated tree populations in localized areas
406 (Fig. 7). The existence of such refugia is subject of a long-standing discussion in the palaeoecology
407 community (Bennett et al., 1991; Petit et al., 2003; Tzedakis et al., 2013). Such refugia are often
408 linked to favourable microclimates that may occupy areas too small to be resolved by climate and
409 vegetation models (Dobrowski, 2011; Rull, 2010; Timbrell et al., 2024; Vercauteren et al., 2013).

410 The ecological changes associated with interstadial, stadial, and full glacial climate conditions are
411 most drastic and diverse in Eastern Europe (Fig. 5–7). Both vegetation models predict several states
412 of forest cover coexist during all stages of the Last Glacial. However, these observations are difficult
413 to validate using pollen data due to the lack of suitable archives in Eastern Europe. North of 50°N and
414 in the Carpathian Mountains, model-based and pollen-based reconstructions show a high
415 agreement. During intermediate to warm conditions (i.e., GI-14) forests dominate the landscape.
416 Climatic cooling during MIS 3 and 2 induces a gradual decline in the Eastern European forests in a
417 clearly discernible latitudinal gradient, resulting in a widespread distribution of tundra in the
418 northern parts and forest-tundra or forest-steppe ecotones further south (i.e., closer to 50°N).
419 Further south, in the Pontic–Caspian region (i.e., the area stretching from north of the Black Sea
420 eastward to the Caspian Sea), such forest-tundra or forest-steppe ecotones characterise the
421 interstadial vegetation. By the time of the LGM, these forest populations have been largely replaced
422 by open landscapes akin to the modern Eurasian steppe.

423

424 **4.2. Proxy-model mismatch**

425 On a continental scale, the different forest-cover reconstructions show a remarkable similarity in the
426 temporal dynamics of forest cover during the Last Glacial. Overall, all methods capture the long-term
427 sequence of forest expansions and retractions associated with climatic variability during MIS 4–2.
428 While there is some variability that can be attributed to Greenland Stadials and Interstadials, the
429 limited temporal resolution impedes a more extensive analysis of the impact of the abrupt climatic
430 transitions on the forest populations in Europe.

431 On regional scales, proxy-model agreement is highest in Eastern Europe, the Iberian Peninsula, and
432 the Middle East. In turn, the agreement between methods is weak in Western and Central Europe as
433 well as the central Mediterranean region, where models suggest moderate to high forest cover,
434 while pollen data indicate widespread tundra and/or steppe landscapes. Previous studies, both on
435 pollen data (Bigelow et al., 2003; Binney et al., 2017; Tarasov et al., 2000) and model reconstructions
436 (Harrison and Prentice, 2003; Strandberg et al., 2011), have observed similar forest-cover
437 distributions during glacial climates (primarily during the LGM). In particular, these patterns of
438 model-proxy agreement and mismatch have been known to the community (Davis et al., 2024;
439 Kaplan et al., 2016) and are not limited to glacial climates only (Dallmeyer et al., 2023; Marquer et al.,
440 2017; Strandberg et al., 2022).

441 Despite capturing the general trend of forest cover dynamics during the Last Glacial, there exists a
442 fundamental offset in the mean forest-cover reconstructions (Fig. 3). This can inspire very different
443 interpretations of the Last Glacial landscapes, from barren tundra or steppe environments to open
444 (boreal) forests, with wide-ranging consequences for data interpretation, e.g., the inference of
445 ecological preferences of Palaeolithic hunter-gatherer groups. The apparent overrepresentation of
446 trees north of the Alps by vegetation models has been previously reported (Davis et al., 2024; Kaplan
447 et al., 2016) and is not in agreement with the general consensus that Europe was predominantly
448 treeless during the LGM (Bigelow et al., 2003; Binney et al., 2017; Tarasov et al., 2000). It also
449 contradicts our understanding of glacial landscapes in Europe during the Late Pleistocene with
450 regards to large herbivore presence (Ukkonen et al., 2011), aDNA evidence (Willerslev et al., 2014),
451 permafrost presence (Stevens et al., 2025), and speleothem data (Fleitmann et al., 2009; Genty et al.,
452 2010; Staubwasser et al., 2018), which all indicate harsh climatic conditions and a mosaic of tundra,
453 steppe, and open forest environments (Britzius et al., 2024; Holm and Svenning, 2014; Pederzani et
454 al., 2023). At the same time, the comparison of methods in this study suggests that REVEALS
455 reconstructions may underestimate forest cover, predicting mostly tundra and steppe landscapes
456 during all periods of the Last Glacial. This is most apparent in the low magnitude of forest expansions
457 during periods of climate amelioration, when (open) forests (re-)emerged in Central Europe as
458 documented by raw pollen data (Britzius et al., 2024; Fletcher et al., 2010; Kern et al., 2022; Woillard,
459 1978).

460 As stated in the methods section, the most likely explanation for this mismatch lies in the different
461 outputs that all methods generate as well as their interpretation in the context of forest cover. While
462 a unified scheme that allows for a 1-to-1 comparison is unlikely to accommodate for all the
463 intricacies of the different reconstruction methods, it remains essential to be able to compare and
464 validate datasets. For this reason, we investigate the particular limitations of the different methods,
465 briefly discuss how to interpret their respective output in a wider context, and explore potential
466 solutions for future vegetation reconstructions efforts.

467 **4.3. Model limitations**

468 Vegetation models have substantially improved over the last decade and have been successfully
469 applied to answer various research questions on various temporal and spatial scales. Nonetheless,

470 high model-complexity comes at the cost of spatial and/or temporal resolution (Laepplé et al., 2023)
471 and whether a high-complexity or a high-resolution model (or something in-between) is more
472 suitable depends on the research question.

473 Global vegetation models, such as JSBACH (within the MPI-ESM), rely on climatic and climate-related
474 parameters to reconstruct the vegetation on global scales. As such, PFT definitions are relatively
475 broad to reflect all general vegetation types and thus limited in their ability to represent vegetation
476 patterns on regional to local scales. A major advantage of the PFT approach is that it can predict the
477 percentage of land cover, e.g., the percentage of land covered by different types of trees, shrubs,
478 grasses, and bare soil within a grid cell. As such, it represents the actual landscape one would
479 observe, which makes it straightforward to interpret the data. These models often also include the
480 parameterisation of complex processes that affect plant growth, decline, or disturbance, e.g., soil
481 moisture and soil dynamics (le Roux et al., 2013). Many of these parameters and thresholds are
482 necessarily tuned to and validated by modern vegetation data (Dallmeyer et al., 2023) or to a mean
483 climate state that is established for a given time period, such as the LGM (Laepplé et al., 2023).
484 Vegetation models often do not include (mostly) treeless environments such as permafrost soils,
485 peatlands, or wetlands and therefore may not recognize these areas as open vegetation and
486 incorrectly predict a much higher forest cover (Dallmeyer et al., 2023). Considering that permafrost
487 landscapes (Stevens et al., 2025) and wetlands (Čížková et al., 2013) were widespread across Last
488 Glacial Europe, this contributes to the overall overestimation of the forest cover in affected regions.
489 The extent of global ice sheets is often prescribed from reconstructions that can vary a lot and effect
490 the climate variability in particular during time periods with strong fluctuations e.g., during MIS 3
491 (Menviel et al., 2020). This simplification of ice sheets might further contribute to the lack of regional
492 variability observed in models (Laepplé et al., 2023).

493 In light of modern climate change and anthropogenic land-use, the present-day climate-vegetation
494 relationship is increasingly at a disequilibrium (Sandel et al., 2025; Svenning and Sandel, 2013) and
495 thus does not accurately represent the bioclimatic relationships accordingly. Climate or vegetation
496 states in the past may have differed to the point that there exists no (near-)analogue in today's world
497 (Correa-Metrio et al., 2012; Magyari et al., 2014; Williams and Jackson, 2007). Using present-day data
498 for training, calibration, and validation of vegetation models also implies that the calibrated
499 parameters are constant over time (Dallmeyer et al., 2023). However, it has been shown that plant
500 physiological traits are dynamic in response to various factors (e.g., water availability, CO₂, and the
501 ecological context) and vary across species, lineages, and timescales (Becklin et al., 2014; Beerling
502 and Woodward, 1993; Franks et al., 2013). Vegetation models also assume that the palaeovegetation
503 is at an equilibrium with the palaeoclimate, which introduces additional uncertainties when
504 interpreting such data. Lastly, PaleoVeg generates probabilities for the occurrence of all vegetation
505 types within a grid cell. While these probabilities can yield information on forest cover (by summing
506 up the probabilities of all forested vegetation types) the actual vegetation composition remains
507 unknown.

508 **4.4. Pollen data limitations**

509 Pollen data as a proxy for palaeoenvironmental conditions have a long-standing tradition and are one
510 of the major indicators used to reconstruct terrestrial ecosystems. As with all proxy data, pollen
511 archives often provide data at different temporal resolutions, include hiatuses, and/or cover only
512 limited time periods within a study interval. Suitable pollen archives are sparse, and their geographic
513 distribution is highly heterogeneous (Fig. 2), especially on global scales. However, researchers have
514 used the properties of windborne pollen dispersal (>100 km; Robledo-Arnuncio, 2011) and
515 deposition to their advantage as pollen archives capture the vegetation signal from a wider region,
516 which often compensates for the lack of spatial coverage. Nonetheless, all future reconstructions

517 would benefit from the emergence of new well-dated pollen datasets with a high temporal
518 resolution.

519 Early on, researcher have identified non-linear relationships between fossil pollen data and the
520 palaeovegetation (Parsons and Prentice, 1981; Prentice, 1985). First and foremost, wind-pollinated
521 plants produce many more pollen grains than insect-pollinated plants and thus are drastically
522 overrepresented in pollen data. But even within the group of wind-pollinated plants, production
523 estimates can vary by a factor of >1000. Variability within a genus or family is reported as high as a
524 factor of ~100 (Githumbi et al., 2022; Schild et al., 2025). These effects may be further exacerbated
525 by different preservation capabilities post-deposition (Havinga, 1967; Li et al., 2005). The range of
526 wind-dispersed pollen grains is also species-specific (pollen morphology and density) and varies with
527 the local topography and wind patterns (Markgraf, 1980; Niklas, 1985). Modern vegetation
528 reconstruction techniques aim to address these non-linear relationships by including a range of
529 assumptions (Chevalier et al., 2020; Davis et al., 2024; Fyfe et al., 2010; Prentice et al., 1996; Sugita,
530 2007; Theuerkauf and Couwenberg, 2018).

531 Overall, studies have hinted that vegetation shifts often appear too strong in pollen-based methods.
532 The overrepresentation of tree cover during the Holocene is typically attributed to the much higher
533 (several orders of magnitude) pollen productivity of trees per area. Modern vegetation
534 reconstruction techniques account for this (Binney et al., 2017; Serge et al., 2023), but the very same
535 approach can lead to an underrepresentation of tree cover during glacial periods (Kern et al., 2025).
536 The fact that pollen-productivity estimates are based on modern interglacial conditions and
537 therefore less accurate for different climate states such as during the Last Glacial might be a major
538 component of this uncertainty (Dallmeyer et al., 2025).

539 A major restriction of pollen-based reconstructions (including REVEALS and Biomisation) is that they
540 implicitly assume complete (100%) vegetation cover, because they can only represent the vegetation
541 that is present and not the lack thereof. However, during the Last Glacial period, large areas of
542 Europe were either approaching or had already surpassed the environmental limits of vegetation
543 growth, especially in the higher latitudes, at high altitudes, and in close vicinity to ice sheets (Allen et
544 al., 2010; Bigelow et al., 2003; Davis et al., 2024). Consequently, the assumption that these areas
545 were nearly completely covered by vegetation does not hold and pollen-based data should be
546 interpreted carefully as they might only represent a small fraction of the actual landscape.

547 Lastly, the characterisation and differentiation of (sub-)biomes (e.g., shrub tundra and cushion-forb
548 tundra) is often based on the exact species (e.g., *Betula* or *Salix*) and/or growth form (e.g., *Corylus*
549 *avellana* or *Alnus* spp.) of certain indicator taxa. Often it is near-impossible to distinguish fossil pollen
550 data on a species level, which may lead to erroneous assumptions about the palaeoenvironment
551 when interpreting and incorporating such data. Despite the taphonomic and depositional biases,
552 pollen data provide a snapshot of the palaeovegetation at a given point in time that encapsulated all
553 factors that have affected the vegetation, which almost always extent beyond climatic factors alone.

554 **4.5. Non-climatic factors that impacted vegetation patterns**

555 Ecosystems are highly complex and the sheer number of external factors that influence its dynamics
556 cannot be reliably accounted for in vegetation reconstructions. The challenge hereby is two-fold: (a)
557 incorporating these factors into vegetations models, and (b) disentangling the proxy data signal, in
558 which these external factors are implicitly embedded.

559 In recent times, the primary external factor that influenced vegetation patterns, density, structure,
560 and biodiversity has been human land use, which has exponentially increased since the onset of
561 farming practices in the Early Holocene (Ellis et al., 2013). Before that, the human impact on Last

562 Glacial environments was comparably low and limited to two processes: a direct impact by the usage
563 of fire and an indirect impact through hunting of medium to large herbivores. The magnitude of
564 impact from both processes is naturally tied to the overall human population, which seems to have
565 gradually – although not linearly – increased in Europe during the Late Pleistocene (Schmidt et al.,
566 2021; Tallavaara et al., 2015).

567 Wildfires have the potential to transform landscapes on large scales. But due to the cold climatic
568 conditions and reduced vegetation cover, natural wildfire activity during the Last Glacial in Europe
569 was comparably lower than today (Daniau et al., 2010; Haas et al., 2023). Before the advent of
570 agriculture during the early Holocene and the targeted use of fire to clear patches of land, human-
571 caused fires have likely been accidental. Anthropogenically caused fires likely have had a substantial
572 impact on the post-LGM vegetation (Kaplan et al., 2016) and concrete evidence for large scale
573 impacts on ecosystems exists from the Late Glacial and early Holocene period onwards (Connor et
574 al., 2019; Dietze et al., 2018; Feurdean et al., 2020; Robin and Nelle, 2014). Prior to the LGM,
575 evidence for the use of fire is abundant, but the ecological impact was very local (Nikulina et al.,
576 2024, 2025; Roebroeks et al., 2021).

577 Hunting of large herbivores, thereby reducing their distribution and density, by Neanderthals and
578 anatomically modern humans has influenced ecosystems on regional scales (Nikulina et al., 2024,
579 2025; Sandom et al., 2014). Recent studies have demonstrated that the abundance and diversity of
580 large herbivore strongly decreased after the arrival of modern humans in Europe ca. 50 ka BP
581 (Bergman et al., 2023; Smith et al., 2018). Prior to that, European ecosystems were characterised by
582 much higher proportions of open a light-woodland (Pearce et al., 2023) and habitat mosaics
583 (Johnson, 2009), which are directly linked to the influence of large herbivores on vegetation structure
584 and composition (Davoli et al., 2024; Svenning et al., 2024). Herbivorous megafauna engineer
585 ecosystems globally by increasing heterogeneity in plant cover and biomes as well as decreasing
586 plant biomass and -cover through consumption, trampling and wallowing (Johnson, 2009; Trepel et
587 al., 2024). Moreover, fire activity has increased in grassy ecosystems in response to herbivore
588 extinction – these grassy ecosystems have covered a larger area during the Last Glacial than today
589 (Karp et al., 2021) – and plant taxa that coevolved with large herbivores have disappeared (Davoli et
590 al., 2024; Johnson, 2009). The global decline of large herbivores in the context of the arrival of
591 modern humans also has broader implications for anthropogenic climate change and biodiversity
592 (Pringle et al., 2023; Svenning et al., 2024).

593 **4.6. Implications for understanding human dispersal processes**

594 In terms of human-environmental interaction, environmental preferences, and derived models of
595 human dispersal (e.g., Shao et al., 2024), it makes a great difference whether a non-, medium- or
596 high-forested landscape is assumed. When compared to the overall mean, the dispersal of modern
597 humans between 60 and 43 ka is connected to a period of relatively high forest cover (Fig. 4).
598 Absolute estimates, however, vary between 15 % and 70 % (Fig. 3) and are thus too broad for
599 meaningful statements on ecological preferences. Nonetheless, it is conspicuous that one of the
600 most pronounced demographic turnovers in Europe – namely the disappearance of the last
601 Neanderthals alongside the pre-Aurignacian anatomically modern humans and the dispersal of the
602 Aurignacian population at around 43 ka (Posth et al., 2023), coincides with a transition from a
603 relatively high to a relatively low forest cover in the vegetation estimates with particularly
604 inconsistent signals from the different models (Fig. 4). Despite the inconsistencies between different
605 models for the individual time bins, the general trend indicates that a profound change in the
606 European vegetation from rather forested to rather open landscapes with all its ecological
607 consequences contributed to this demographic shift. The continued decrease in relative forest cover

608 indicates an increase in steppe or tundra environments, which may also support the idea of a
609 decrease in net primary production (Maier et al., 2022).

610 During the LGM, the results indicate a roughly binary division of the European landscape (Fig. 7).
611 From the Cote d'Azur over the Italian Peninsula and the Balkans up to the Eastern European steppe,
612 intermediate to above-average forest cover is indicated, while the Iberian Peninsula (except the
613 Atlantic coast), Western, and Central Europe north of the Alps and Carpathians are characterised by
614 below-average values. Interestingly, this ecological boundary coincides with the boundary between
615 the Epigravettian in the former area, and the Solutrean in the latter. The finding that LGM settlement
616 areas of the Epigravettian seem to be located in intermediate to above-average forested areas while,
617 at the same time, being (Maier et al., 2016) situated well within the zone of continuous permafrost
618 (Stevens et al., 2025), challenges our perception of the nature of these refugial areas and
619 concomitant human adaptation (Maier et al., 2016). Given the right conditions in favourable
620 microclimate, boreal trees can grow in continuous permafrost, let alone the option of small isolated
621 pockets of discontinuous permafrost that could have also occurred. Maier et al., (2016), PaleoVeg,
622 and JSBACH agree that the western coast of the Iberian Peninsula maintained relatively mild climates
623 and lightly forested areas – the only area in Western Europe that also maintained stable population
624 numbers and densities throughout the climatic developments towards the LGM (Maier et al., 2016;
625 Maier and Zimmermann, 2017).

626 5. Conclusions

627 Palaeovegetation reconstructions are an important aspect of understanding past ecosystems and
628 how they have shaped demographic developments of hunter-gatherers across Europe during the Last
629 Glacial period. In this study, we show that exploiting more than one dataset is required to fully utilise
630 the potential of palaeovegetation reconstructions.

631 Overall, we highlight that all methods used in this study are capable of accurately reconstructing the
632 changing vegetation throughout the late Last Glacial (70–20 ka BP) on continental scales. Irrespective
633 of the method used, the general vegetation patterns follow the climatic variability observed in this
634 period and thus indicate higher forest cover during early MIS 3 that gradually decreases to a
635 minimum during the LGM. On local scales, the reconstructions may vary due to inherent
636 uncertainties within all of the methods. Importantly, we show that absolute values of forest cover
637 can vary by up to 40 % depending on the method and can therefore not be interpreted at face value.
638 This is likely related to the lack of a clear definition of forest cover as well as the widely different
639 outputs generated by each method.

640 The implications of these findings for the use of vegetation reconstructions with regards to
641 demographic developments of humans in Europe during the Last Glacial are highly significant:
642 Depending on the chosen method, a population of hunter-gatherers would have lived in a boreal
643 forest environment or an arctic tundra with minimal vegetation. Instead, we highly recommend using
644 relative measures and avoiding absolute values when discussing forest cover. Relative decreases in
645 forest cover can independently of the method and unequivocally be interpreted as an opening of the
646 landscape and vice versa. In cases where the absolute forest cover is strictly necessary, employing
647 multiple methods and combining results can lead to a much more robust signal. However, in this case
648 it is imperative to keep the individual method-specific limitations in mind when interpreting the
649 results.

650 Pollen-based methods present snapshots of past vegetation states reflecting the local to regional
651 interplay between different factors, such as climate, soil conditions, and flora-fauna interaction.
652 While they typically represent a wider area, they remain limited in their geographic coverage due to
653 the scarcity of available datasets. Therefore, pollen-based data are ideally suited to accompany e.g.,

654 archaeological data at specific points in time. Concerning the vegetation models in this study, JSBACH
655 offers a considerably higher complexity compared to PaleoVeg, but lacks representation of
656 permafrost soils, peatlands, and wetlands, which were abundant during the Last Glacial. PaleoVeg
657 can be applied at the spatial resolution of the input predictor layers, which enables easier access to
658 high resolution vegetation data and thus offers valuable insights when input data and model
659 parameters are well constrained. These palaeovegetation models provide continuous data in space
660 and time, making them powerful tools to identify broad-scale patterns such as ecosystem dynamics,
661 migration pathways, and habitat connectivity. Such continuous data are also extremely valuable to
662 inform suitability landscapes used to model human dispersal processes, such as the human existence
663 potential (HEP) included in the Our Way Model Framework (e.g., Klein et al., 2021; Shao et al., 2024).

664 Future research will continue to improve the output of individual methods, by e.g., increasing the
665 number of pollen records available, improving the accuracy of external parameters (such as the RPP),
666 increasing the spatial resolution of vegetation models (e.g., by generating higher-resolution
667 palaeoclimate data), and using more accurate calibrations of various processes within vegetation
668 models. Nonetheless, combining methods will always provide a more comprehensive view of the
669 palaeovegetation than a single method ever will. A promising avenue of research lies in the
670 integration of pollen-based data into a vegetation model using data assimilation. That way, real
671 world data from pollen archives would inform and improve vegetation models directly, rather than
672 just being compared to at a later stage.

673 To facilitate the process of data exploration and interpretation, we introduce PALVEG 2.0
674 (https://oakern.shinyapps.io/palveg_v2/), a visualisation framework to quickly glance over the data
675 generated in this study. The aim of PALVEG 2.0 is to help researchers identify areas/intervals of
676 interest, explore the data in detail, and to reduce the time and effort required to get a first glance on
677 how the palaeovegetation might have looked like based on the four different methods used in this
678 study.

679 Data availability

680 All datasets generated in this study are available in the Zenodo database
681 (<https://doi.org/10.5281/zenodo.19630750>; Kern et al., 2026).

682 Acknowledgements

683 This work is supported by the European Research Council (MEMELAND, Grant agreement ID:
684 101166850, doi.org/10.3030/101166850). Views and opinions expressed are however those of the
685 author(s) only and do not necessarily reflect those of the European Union or the European Research
686 Council Executive Agency. Neither the European Union nor the granting authority can be held
687 responsible for them.

688 The project "HESCOR" is receiving funding from the programme "Profilbildung 2022", an initiative of
689 the Ministry of Culture and Science of the State of North-Rhine Westphalia, Germany (HESCOR PB22-
690 081). The sole responsibility for the content of this publication lies with the authors.

691 A.D. would like to thank the Federal Ministry of Research, Technology and Space (BMFTR) for its
692 support under the "Research for Sustainability" (FONA) initiative through the PalMod Phase III
693 project (Grant number 01LP2306A).

694

695 **References**

- 696 Alkama, R. and Cescatti, A.: Biophysical climate impacts of recent changes in global forest cover,
697 *Science*, 351, 600–604, <https://doi.org/10.1126/science.aac8083>, 2016.
- 698 Allen, J. R. M., Watts, W. A., and Huntley, B.: Weichselian palynostratigraphy, palaeovegetation and
699 palaeoenvironment; the record from Lago Grande di Monticchio, southern Italy, *Quaternary*
700 *International*, 73–74, 91–110, [https://doi.org/10.1016/S1040-6182\(00\)00067-7](https://doi.org/10.1016/S1040-6182(00)00067-7), 2000.
- 701 Allen, J. R. M., Hickler, T., Singarayer, J. S., Sykes, M. T., Valdes, P. J., and Huntley, B.: Last glacial
702 vegetation of northern Eurasia, *Quaternary Science Reviews*, 29, 2604–2618,
703 <https://doi.org/10.1016/j.quascirev.2010.05.031>, 2010.
- 704 Arpe, K., Leroy, S. a. G., and Mikolajewicz, U.: A comparison of climate simulations for the last glacial
705 maximum with three different versions of the ECHAM model and implications for summer-green tree
706 refugia, *Climate of the Past*, 7, 91–114, <https://doi.org/10.5194/cp-7-91-2011>, 2011.
- 707 Bartlein, P. J., Harrison, S. P., Brewer, S., Connor, S., Davis, B. A. S., Gajewski, K., Guiot, J., Harrison-
708 Prentice, T. I., Henderson, A., Peyron, O., Prentice, I. C., Scholze, M., Seppä, H., Shuman, B., Sugita, S.,
709 Thompson, R. S., Viau, A. E., Williams, J., and Wu, H.: Pollen-based continental climate
710 reconstructions at 6 and 21 ka: a global synthesis, *Clim Dyn*, 37, 775–802,
711 <https://doi.org/10.1007/s00382-010-0904-1>, 2011.
- 712 Becklin, K. M., Medeiros, J. S., Sale, K. R., and Ward, J. K.: Evolutionary history underlies plant
713 physiological responses to global change since the last glacial maximum, *Ecol Lett*, 17, 691–699,
714 <https://doi.org/10.1111/ele.12271>, 2014.
- 715 Beerling, D. J. and Woodward, F. I.: Ecophysiological responses of plants to global environmental
716 change since the Last Glacial Maximum, *New Phytol*, 125, 641–648, <https://doi.org/10.1111/j.1469-8137.1993.tb03914.x>, 1993.
- 718 Bennett, K. D., Tzedakis, P. C., and Willis, K. J.: Quaternary Refugia of North European Trees, *Journal*
719 *of Biogeography*, 18, 103–115, <https://doi.org/10.2307/2845248>, 1991.
- 720 Bergman, J., Pedersen, R. Ø., Lundgren, E. J., Lemoine, R. T., Monsarrat, S., Pearce, E. A., Schierup, M.
721 H., and Svenning, J.-C.: Worldwide Late Pleistocene and Early Holocene population declines in extant
722 megafauna are associated with *Homo sapiens* expansion rather than climate change, *Nat Commun*,
723 14, 7679, <https://doi.org/10.1038/s41467-023-43426-5>, 2023.
- 724 Beyer, R. M., Krapp, M., and Manica, A.: High-resolution terrestrial climate, bioclimate and
725 vegetation for the last 120,000 years, *Sci Data*, 7, 236, <https://doi.org/10.1038/s41597-020-0552-1>,
726 2020.
- 727 Bigelow, N. H., Brubaker, L. B., Edwards, M. E., Harrison, S. P., Prentice, I. C., Anderson, P. M.,
728 Andreev, A. A., Bartlein, P. J., Christensen, T. R., Cramer, W., Kaplan, J. O., Lozhkin, A. V., Matveyeva,
729 N. V., Murray, D. F., McGuire, A. D., Razzhivin, V. Y., Ritchie, J. C., Smith, B., Walker, D. A., Gajewski,
730 K., Wolf, V., Holmqvist, B. H., Igarashi, Y., Kremenetskii, K., Paus, A., Pisaric, M. F. J., and Volkova, V.
731 S.: Climate change and Arctic ecosystems: 1. Vegetation changes north of 55°N between the last
732 glacial maximum, mid-Holocene, and present, *Journal of Geophysical Research: Atmospheres*, 108,
733 <https://doi.org/10.1029/2002JD002558>, 2003.
- 734 Binney, H., Edwards, M., Macias-Fauria, M., Lozhkin, A., Anderson, P., Kaplan, J. O., Andreev, A.,
735 Bezrukova, E., Blyakharchuk, T., Jankovska, V., Khazina, I., Krivonogov, S., Kremenetski, K., Nield, J.,
736 Novenko, E., Ryabogina, N., Solovieva, N., Willis, K., and Zernitskaya, V.: Vegetation of Eurasia from

737 the last glacial maximum to present: Key biogeographic patterns, *Quaternary Science Reviews*, 157,
738 80–97, <https://doi.org/10.1016/j.quascirev.2016.11.022>, 2017.

739 Bright, R. M., Zhao, K., Jackson, R. B., and Cherubini, F.: Quantifying surface albedo and other direct
740 biogeophysical climate forcings of forestry activities, *Global Change Biology*, 21, 3246–3266,
741 <https://doi.org/10.1111/gcb.12951>, 2015.

742 Britzius, S., Dreher, F., Maisel, P., and Sirocko, F.: Vegetation Patterns during the Last 132,000 Years:
743 A Synthesis from Twelve Eifel Maar Sediment Cores (Germany): The ELSA-23-Pollen-Stack,
744 *Quaternary*, 7, 8, <https://doi.org/10.3390/quat7010008>, 2024.

745 Brovkin, V., Raddatz, T., Reick, C. H., Claussen, M., and Gayler, V.: Global biogeophysical interactions
746 between forest and climate, *Geophysical Research Letters*, 36,
747 <https://doi.org/10.1029/2009GL037543>, 2009.

748 Chevalier, M., Davis, B. A. S., Heiri, O., Seppä, H., Chase, B. M., Gajewski, K., Lacourse, T., Telford, R.
749 J., Finsinger, W., Guiot, J., Köhler, N., Maezumi, S. Y., Tipton, J. R., Carter, V. A., Brussel, T., Phelps, L. N.,
750 Dawson, A., Zanon, M., Vallé, F., Nolan, C., Mauri, A., de Vernal, A., Izumi, K., Holmström, L.,
751 Marsicek, J., Goring, S., Sommer, P. S., Chaput, M., and Kupriyanov, D.: Pollen-based climate
752 reconstruction techniques for late Quaternary studies, *Earth-Science Reviews*, 210, 103384,
753 <https://doi.org/10.1016/j.earscirev.2020.103384>, 2020.

754 Čížková, H., Květ, J., Comín, F. A., Laiho, R., Pokorný, J., and Pithart, D.: Actual state of European
755 wetlands and their possible future in the context of global climate change, *Aquat Sci*, 75, 3–26,
756 <https://doi.org/10.1007/s00027-011-0233-4>, 2013.

757 Connor, S. E., Vannièrè, B., Colombaroli, D., Anderson, R. S., Carrión, J. S., Ejarque, A., Gil Romera, G.,
758 González-Sampériz, P., Hofer, D., Morales-Molino, C., Revelles, J., Schneider, H., van der Knaap, W.
759 O., van Leeuwen, J. F., and Woodbridge, J.: Humans take control of fire-driven diversity changes in
760 Mediterranean Iberia’s vegetation during the mid–late Holocene, *The Holocene*, 29, 886–901,
761 <https://doi.org/10.1177/0959683619826652>, 2019.

762 Correa-Metrio, A., Bush, M. B., Cabrera, K. R., Sully, S., Brenner, M., Hodell, D. A., Escobar, J., and
763 Guilderson, T.: Rapid climate change and no-analog vegetation in lowland Central America during the
764 last 86,000 years, *Quaternary Science Reviews*, 38, 63–75,
765 <https://doi.org/10.1016/j.quascirev.2012.01.025>, 2012.

766 Dallmeyer, A., Claussen, M., and Brovkin, V.: Harmonising plant functional type distributions for
767 evaluating Earth system models, *Climate of the Past*, 15, 335–366, <https://doi.org/10.5194/cp-15-335-2019>, 2019.

769 Dallmeyer, A., Kleinen, T., Claussen, M., Weitzel, N., Cao, X., and Herzschuh, U.: The deglacial forest
770 conundrum, *Nat Commun*, 13, 6035, <https://doi.org/10.1038/s41467-022-33646-6>, 2022.

771 Dallmeyer, A., Poska, A., Marquer, L., Seim, A., and Gaillard, M.-J.: The challenge of comparing pollen-
772 based quantitative vegetation reconstructions with outputs from vegetation models – a European
773 perspective, *Climate of the Past*, 19, 1531–1557, <https://doi.org/10.5194/cp-19-1531-2023>, 2023.

774 Dallmeyer, A., Weitzel, N., Schild, L., Herzschuh, U., Kleinen, T., and Claussen, M.: Unravelling the tree
775 cover dynamics over the last 20,000 years on the Northern Hemisphere, *EGUsphere*, 1–48,
776 <https://doi.org/10.5194/egusphere-2025-6393>, 2025.

777 Daniau, A.-L., Harrison, S. P., and Bartlein, P. J.: Fire regimes during the Last Glacial, *Quaternary
778 Science Reviews*, 29, 2918–2930, <https://doi.org/10.1016/j.quascirev.2009.11.008>, 2010.

779 Davis, B. A. S., Fasel, M., Kaplan, J. O., Russo, E., and Burke, A.: The climate and vegetation of Europe,
780 northern Africa, and the Middle East during the Last Glacial Maximum
781 (21 000 yr BP) based on pollen data, *Climate of the Past*, 20, 1939–1988,
782 <https://doi.org/10.5194/cp-20-1939-2024>, 2024.

783 Davoli, M., Monsarrat, S., Pedersen, R. Ø., Scussolini, P., Karger, D. N., Normand, S., and Svenning, J.-
784 C.: Megafauna diversity and functional declines in Europe from the Last Interglacial to the present,
785 *Global Ecology and Biogeography*, 33, 34–47, <https://doi.org/10.1111/geb.13778>, 2024.

786 De Lombaerde, E., Vangansbeke, P., Lenoir, J., Van Meerbeek, K., Lembrechts, J., Rodríguez-Sánchez,
787 F., Luoto, M., Scheffers, B., Haesen, S., Aalto, J., Christiansen, D. M., De Pauw, K., Depauw, L.,
788 Govaert, S., Greiser, C., Hampe, A., Hylander, K., Klings, D., Koelemeijer, I., Meeussen, C., Ogée, J.,
789 Sanczuk, P., Vanneste, T., Zellweger, F., Baeten, L., and De Frenne, P.: Maintaining forest cover to
790 enhance temperature buffering under future climate change, *Science of The Total Environment*, 810,
791 151338, <https://doi.org/10.1016/j.scitotenv.2021.151338>, 2022.

792 Dietze, E., Theuerkauf, M., Bloom, K., Brauer, A., Dörfler, W., Feeser, I., Feurdean, A., Gedminienė, L.,
793 Giesecke, T., Jahns, S., Karpińska-Kończak, M., Kończak, P., Lamentowicz, M., Latałowa, M., Marcisz,
794 K., Obremaska, M., Pędziszewska, A., Poska, A., Rehfeld, K., Stančikaitė, M., Stivrins, N., Święta-
795 Musznicka, J., Szal, M., Vassiljev, J., Veski, S., Wacnik, A., Weisbrodt, D., Wiethold, J., Vannière, B.,
796 and Słowiński, M.: Holocene fire activity during low-natural flammability periods reveals scale-
797 dependent cultural human-fire relationships in Europe, *Quaternary Science Reviews*, 201, 44–56,
798 <https://doi.org/10.1016/j.quascirev.2018.10.005>, 2018.

799 Dobrowski, S. Z.: A climatic basis for microrefugia: the influence of terrain on climate, *Global Change*
800 *Biology*, 17, 1022–1035, <https://doi.org/10.1111/j.1365-2486.2010.02263.x>, 2011.

801 Duque-Villegas, M., Claussen, M., Kleinen, T., Bader, J., and Reick, C. H.: Pattern scaling of simulated
802 vegetation change in northern Africa during glacial cycles, *Climate of the Past*, 21, 773–794,
803 <https://doi.org/10.5194/cp-21-773-2025>, 2025.

804 Ehlers, J., Gibbard, P. L., and Hughes, P. D.: *Quaternary Glaciations - Extent and Chronology A Closer*
805 *Look*, Elsevier, 2011.

806 Ellis, E. C., Kaplan, J. O., Fuller, D. Q., Vavrus, S., Klein Goldewijk, K., and Verburg, P. H.: Used planet: A
807 global history, *Proceedings of the National Academy of Sciences*, 110, 7978–7985,
808 <https://doi.org/10.1073/pnas.1217241110>, 2013.

809 Feurdean, A., Vannière, B., Finsinger, W., Warren, D., Connor, S. C., Forrest, M., Liakka, J., Panait, A.,
810 Werner, C., Andrič, M., Bobek, P., Carter, V. A., Davis, B., Diaconu, A.-C., Dietze, E., Feeser, I.,
811 Florescu, G., Gałka, M., Giesecke, T., Jahns, S., Jamrichová, E., Kajukało, K., Kaplan, J., Karpińska-
812 Kończak, M., Kończak, P., Kuneš, P., Kupriyanov, D., Lamentowicz, M., Lemmen, C., Magyari, E. K.,
813 Marcisz, K., Marinova, E., Niamir, A., Novenko, E., Obremaska, M., Pędziszewska, A., Pfeiffer, M.,
814 Poska, A., Rösch, M., Słowiński, M., Stančikaitė, M., Szal, M., Święta-Musznicka, J., Tanțău, I.,
815 Theuerkauf, M., Tonkov, S., Valkó, O., Vassiljev, J., Veski, S., Vincze, I., Wacnik, A., Wiethold, J., and
816 Hickler, T.: Fire hazard modulation by long-term dynamics in land cover and dominant forest type in
817 eastern and central Europe, *Biogeosciences*, 17, 1213–1230, [https://doi.org/10.5194/bg-17-1213-](https://doi.org/10.5194/bg-17-1213-2020)
818 2020, 2020.

819 Fick, S. E. and Hijmans, R. J.: WorldClim 2: new 1-km spatial resolution climate surfaces for global
820 land areas, *International Journal of Climatology*, 37, 4302–4315, <https://doi.org/10.1002/joc.5086>,
821 2017.

822 Fleitmann, D., Cheng, H., Badertscher, S., Edwards, R. L., Mudelsee, M., Gökürk, O. M., Fankhauser,
823 A., Pickering, R., Raible, C. C., Matter, A., Kramers, J., and Tüysüz, O.: Timing and climatic impact of
824 Greenland interstadials recorded in stalagmites from northern Turkey, *Geophysical Research Letters*,
825 36, <https://doi.org/10.1029/2009GL040050>, 2009.

826 Fletcher, W. J., Sánchez Goñi, M. F., Allen, J. R. M., Cheddadi, R., Combourieu-Nebout, N., Huntley, B.,
827 Lawson, I., Londeix, L., Magri, D., Margari, V., Müller, U. C., Naughton, F., Novenko, E., Roucoux, K.,
828 and Tzedakis, P. C.: Millennial-scale variability during the last glacial in vegetation records from
829 Europe, *Quaternary Science Reviews*, 29, 2839–2864,
830 <https://doi.org/10.1016/j.quascirev.2009.11.015>, 2010.

831 Franks, P. J., Adams, M. A., Amthor, J. S., Barbour, M. M., Berry, J. A., Ellsworth, D. S., Farquhar, G. D.,
832 Ghannoum, O., Lloyd, J., McDowell, N., Norby, R. J., Tissue, D. T., and von Caemmerer, S.: Sensitivity
833 of plants to changing atmospheric CO₂ concentration: from the geological past to the next century,
834 *New Phytologist*, 197, 1077–1094, <https://doi.org/10.1111/nph.12104>, 2013.

835 Fyfe, R., Roberts, N., and Woodbridge, J.: A pollen-based pseudobiomisation approach to
836 anthropogenic land-cover change, *The Holocene*, 20, 1165–1171,
837 <https://doi.org/10.1177/0959683610369509>, 2010.

838 Genty, D., Combourieu-Nebout, N., Peyron, O., Blamart, D., Wainer, K., Mansuri, F., Ghaleb, B.,
839 Isabello, L., Dormoy, I., and Von Grafenstein, U.: Isotopic characterization of rapid climatic events
840 during OIS3 and OIS4 in Villars Cave stalagmites (SW-France) and correlation with Atlantic and
841 Mediterranean pollen records, *Quaternary Science Reviews*, 29, 2799–2820,
842 <https://doi.org/10.1016/j.quascirev.2010.06.035>, 2010.

843 Giorgino, T.: Computing and Visualizing Dynamic Time Warping Alignments in R: The dtw Package,
844 *Journal of Statistical Software*, 31, 1–24, <https://doi.org/10.18637/jss.v031.i07>, 2009.

845 Githumbi, E., Fyfe, R., Gaillard, M.-J., Trondman, A.-K., Mazier, F., Nielsen, A.-B., Poska, A., Sugita, S.,
846 Woodbridge, J., Azuara, J., Feurdean, A., Grindean, R., Lebreton, V., Marquer, L., Nebout-
847 Combourieu, N., Stančikaitė, M., Tanțău, I., Tonkov, S., Shumilovskikh, L., and LandClimII data
848 contributors: European pollen-based REVEALS land-cover reconstructions for the Holocene:
849 methodology, mapping and potentials, *Earth System Science Data*, 14, 1581–1619,
850 <https://doi.org/10.5194/essd-14-1581-2022>, 2022.

851 Haas, O., Prentice, I. C., and Harrison, S. P.: The response of wildfire regimes to Last Glacial Maximum
852 carbon dioxide and climate, *Biogeosciences*, 20, 3981–3995, [https://doi.org/10.5194/bg-20-3981-](https://doi.org/10.5194/bg-20-3981-2023)
853 2023, 2023.

854 Hallett, E. Y., Leonardi, M., Cerasoni, J. N., Will, M., Beyer, R., Krapp, M., Kandel, A. W., Manica, A.,
855 and Scerri, E. M. L.: Major expansion in the human niche preceded out of Africa dispersal, *Nature*, 1–
856 7, <https://doi.org/10.1038/s41586-025-09154-0>, 2025.

857 Hansen, M. C., Potapov, P. V., Moore, R., Hancher, M., Turubanova, S. A., Tyukavina, A., Thau, D.,
858 Stehman, S. V., Goetz, S. J., Loveland, T. R., Kommareddy, A., Egorov, A., Chini, L., Justice, C. O., and
859 Townshend, J. R. G.: High-Resolution Global Maps of 21st-Century Forest Cover Change, *Science*, 342,
860 850–853, <https://doi.org/10.1126/science.1244693>, 2013.

861 Harrison, S. P. and Prentice, C. I.: Climate and CO₂ controls on global vegetation distribution at the
862 last glacial maximum: analysis based on palaeovegetation data, biome modelling and palaeoclimate
863 simulations, *Global Change Biology*, 9, 983–1004, <https://doi.org/10.1046/j.1365-2486.2003.00640.x>,
864 2003.

865 Harvati, K., Röding, C., Bosman, A. M., Karakostis, F. A., Grün, R., Stringer, C., Karkanas, P., Thompson,
866 N. C., Koutoulidis, V., Mouloupoulos, L. A., Gorgoulis, V. G., and Kouloukoussa, M.: Apidima Cave
867 fossils provide earliest evidence of *Homo sapiens* in Eurasia, *Nature*, 571, 500–504,
868 <https://doi.org/10.1038/s41586-019-1376-z>, 2019.

869 Havinga, A. J.: Palynology and pollen preservation, *Review of Palaeobotany and Palynology*, 2, 81–98,
870 [https://doi.org/10.1016/0034-6667\(67\)90138-8](https://doi.org/10.1016/0034-6667(67)90138-8), 1967.

871 Hershkovitz, I., Weber, G. W., Quam, R., Duval, M., Grün, R., Kinsley, L., Ayalon, A., Bar-Matthews,
872 M., Valladas, H., Mercier, N., Arsuaga, J. L., Martínón-Torres, M., Bermúdez de Castro, J. M., Fornai,
873 C., Martín-Francés, L., Sarig, R., May, H., Krenn, V. A., Slon, V., Rodríguez, L., García, R., Lorenzo, C.,
874 Carretero, J. M., Frumkin, A., Shahack-Gross, R., Bar-Yosef Mayer, D. E., Cui, Y., Wu, X., Peled, N.,
875 Groman-Yaroslavski, I., Weissbrod, L., Yeshurun, R., Tsatskin, A., Zaidner, Y., and Weinstein-Evron,
876 M.: The earliest modern humans outside Africa, *Science*, 359, 456–459,
877 <https://doi.org/10.1126/science.aap8369>, 2018.

878 Holm, S. R. and Svenning, J.-C.: 180,000 Years of Climate Change in Europe: Avifaunal Responses and
879 Vegetation Implications, *PLoS One*, 9, e94021, <https://doi.org/10.1371/journal.pone.0094021>, 2014.

880 Indermühle, A., Monnin, E., Stauffer, B., Stocker, T. F., and Wahlen, M.: Atmospheric CO₂
881 concentration from 60 to 20 kyr BP from the Taylor Dome Ice Core, Antarctica, *Geophysical Research*
882 *Letters*, 27, 735–738, <https://doi.org/10.1029/1999GL010960>, 2000.

883 Johnson, C. n.: Ecological consequences of Late Quaternary extinctions of megafauna, *Proceedings of*
884 *the Royal Society B: Biological Sciences*, 276, 2509–2519, <https://doi.org/10.1098/rspb.2008.1921>,
885 2009.

886 Kaplan, J. O., Pfeiffer, M., Kolen, J. C. A., and Davis, B. A. S.: Large Scale Anthropogenic Reduction of
887 Forest Cover in Last Glacial Maximum Europe, *PLOS ONE*, 11, e0166726,
888 <https://doi.org/10.1371/journal.pone.0166726>, 2016.

889 Karp, A. T., Faith, J. T., Marlon, J. R., and Staver, A. C.: Global response of fire activity to late
890 Quaternary grazer extinctions, *Science*, 374, 1145–1148, <https://doi.org/10.1126/science.abj1580>,
891 2021.

892 Kern, O. A., Koutsodendris, A., Allstädt, F. J., Mächtle, B., Peteet, D. M., Kalaitzidis, S., Christanis, K.,
893 and Pross, J.: A near-continuous record of climate and ecosystem variability in Central Europe during
894 the past 130 kyrs (Marine Isotope Stages 5–1) from Füramoos, southern Germany, *Quaternary*
895 *Science Reviews*, 284, 107505, <https://doi.org/10.1016/j.quascirev.2022.107505>, 2022.

896 Kern, O. A., Maier, A., and Vercauteren, N.: Landscape reconstructions for Europe during the late Last
897 Glacial (60–20 ka BP): a pollen-based REVEALS approach, *Earth System Science Data*, 17, 5997–6023,
898 <https://doi.org/10.5194/essd-17-5997-2025>, 2025.

899 Kern, O. A., Schlüter, P., and Dallmeyer, A.: Vegetation reconstruction datasets (REVEALS,
900 Biomisation, PaleoVeg, JSBACH) for the 70–20 ka BP interval in Europe,
901 <https://doi.org/10.5281/ZENODO.19630750>, 2026.

902 Klein, K., Wegener, C., Schmidt, I., Rostami, M., Ludwig, P., Ulbrich, S., Richter, J., Weniger, G.-C., and
903 Shao, Y.: Human existence potential in Europe during the Last Glacial Maximum, *Quaternary*
904 *International*, 581–582, 7–27, <https://doi.org/10.1016/j.quaint.2020.07.046>, 2021.

905 Laepple, T., Ziegler, E., Weitzel, N., Hébert, R., Ellerhoff, B., Schoch, P., Martrat, B., Bothe, O.,
906 Moreno-Chamarro, E., Chevalier, M., Herbert, A., and Rehfeld, K.: Regional but not global

907 temperature variability underestimated by climate models at supradecadal timescales, *Nat. Geosci.*,
908 16, 958–966, <https://doi.org/10.1038/s41561-023-01299-9>, 2023.

909 Leonardi, M., Hallett, E. Y., Beyer, R., Krapp, M., and Manica, A.: *pastclim 1.2: an R package to easily*
910 *access and use paleoclimatic reconstructions*, *Ecography*, 2023, e06481,
911 <https://doi.org/10.1111/ecog.06481>, 2023.

912 Li, C., Dallmeyer, A., Ni, J., Chevalier, M., Willeit, M., Andreev, A. A., Cao, X., Schild, L., Heim, B.,
913 Wieczorek, M., and Herzschuh, U.: *Global biome changes over the last 21,000 years inferred*
914 *from model–data comparisons*, *Climate of the Past*, 21, 1001–1024, [https://doi.org/10.5194/cp-21-](https://doi.org/10.5194/cp-21-1001-2025)
915 1001-2025, 2025.

916 Li, Y., Xu, Q., Yang, X., Chen, H., and Lu, X.: *Pollen-vegetation relationship and pollen preservation on*
917 *the Northeastern Qinghai-Tibetan Plateau*, *Grana*, 44, 160–171,
918 <https://doi.org/10.1080/00173130500230608>, 2005.

919 Lisiecki, L. E. and Raymo, M. E.: *A Pliocene-Pleistocene stack of 57 globally distributed benthic $\delta^{18}O$*
920 *records*, *Paleoceanography*, 20, <https://doi.org/10.1029/2004PA001071>, 2005.

921 Loveland, T. R., Reed, B. C., Brown, J. F., Ohlen, D. O., Zhu, Z., Yang, L., and Merchant, J. W.:
922 *Development of a global land cover characteristics database and IGBP DISCover from 1 km AVHRR*
923 *data*, *International Journal of Remote Sensing*, 21, 1303–1330,
924 <https://doi.org/10.1080/014311600210191>, 2000.

925 Ludwig, P., Schaffernicht, E. J., Shao, Y., and Pinto, J. G.: *Regional atmospheric circulation over Europe*
926 *during the Last Glacial Maximum and its links to precipitation*, *Journal of Geophysical Research:*
927 *Atmospheres*, 121, 2130–2145, <https://doi.org/10.1002/2015JD024444>, 2016.

928 Magyari, E. K., Kuneš, P., Jakab, G., Sümegi, P., Pelánková, B., Schäbitz, F., Braun, M., and Chytrý, M.:
929 *Late Pleniglacial vegetation in eastern-central Europe: are there modern analogues in Siberia?*,
930 *Quaternary Science Reviews*, 95, 60–79, <https://doi.org/10.1016/j.quascirev.2014.04.020>, 2014.

931 Maier, A. and Zimmermann, A.: *Populations headed south? The Gravettian from a*
932 *palaeodemographic point of view*, *Antiquity*, 91, 573–588, <https://doi.org/10.15184/aqy.2017.37>,
933 2017.

934 Maier, A., Lehmkuhl, F., Ludwig, P., Melles, M., Schmidt, I., Shao, Y., Zeeden, C., and Zimmermann, A.:
935 *Demographic estimates of hunter–gatherers during the Last Glacial Maximum in Europe against the*
936 *background of palaeoenvironmental data*, *Quaternary International*, 425, 49–61,
937 <https://doi.org/10.1016/j.quaint.2016.04.009>, 2016.

938 Maier, A., Stojakowits, P., Mayr, C., Pfeifer, S., Preusser, F., Zolitschka, B., Anghelinu, M., Bobak, D.,
939 Duprat-Oualid, F., Einwögerer, T., Hambach, U., Händel, M., Kaminská, L., Kämpf, L., Łanczont, M.,
940 Lehmkuhl, F., Ludwig, P., Magyari, E., Mroczek, P., Nemergut, A., Nerudová, Z., Niță, L., Polanská, M.,
941 Połtowicz-Bobak, M., Rius, D., Römer, W., Simon, U., Škrdla, P., Újvári, G., and Veres, D.: *Cultural*
942 *evolution and environmental change in Central Europe between 40 and 15 ka*, *Quaternary*
943 *International*, 581–582, 225–240, <https://doi.org/10.1016/j.quaint.2020.09.049>, 2021.

944 Maier, A., Ludwig, P., Zimmermann, A., and Schmidt, I.: *The Sunny Side of the Ice Age: Solar*
945 *Insolation as a Potential Long-Term Pacemaker for Demographic Developments in Europe Between*
946 *43 and 15 ka Ago*, *PaleoAnthropology*, 35-51 Pages, <https://doi.org/10.48738/2022.ISS1.100>, 2022.

947 Maier, A., Tharandt, L., Linsel, F., Krakov, V., and Ludwig, P.: Where the Grass is Greener — Large-
948 Scale Phenological Patterns and Their Explanatory Potential for the Distribution of Paleolithic Hunter-
949 Gatherers in Europe, *J Archaeol Method Theory*, <https://doi.org/10.1007/s10816-023-09628-3>, 2023.

950 Markgraf, V.: Pollen Dispersal in a Mountain Area, *Grana*, 19, 127–146,
951 <https://doi.org/10.1080/00173138009424995>, 1980.

952 Marquer, L., Gaillard, M.-J., Sugita, S., Poska, A., Trondman, A.-K., Mazier, F., Nielsen, A. B., Fyfe, R.
953 M., Jönsson, A. M., Smith, B., Kaplan, J. O., Alenius, T., Birks, H. J. B., Bjune, A. E., Christiansen, J.,
954 Dodson, J., Edwards, K. J., Giesecke, T., Herzschuh, U., Kangur, M., Koff, T., Latałowa, M.,
955 Lechterbeck, J., Olofsson, J., and Seppä, H.: Quantifying the effects of land use and climate on
956 Holocene vegetation in Europe, *Quaternary Science Reviews*, 171, 20–37,
957 <https://doi.org/10.1016/j.quascirev.2017.07.001>, 2017.

958 Mauritsen, T., Bader, J., Becker, T., Behrens, J., Bittner, M., Brokopf, R., Brovkin, V., Claussen, M.,
959 Crueger, T., Esch, M., Fast, I., Fiedler, S., Fläschner, D., Gayler, V., Giorgetta, M., Goll, D. S., Haak, H.,
960 Hagemann, S., Hedemann, C., Hohenegger, C., Ilyina, T., Jahns, T., Jimenéz-de-la-Cuesta, D.,
961 Jungclaus, J., Kleinen, T., Kloster, S., Kracher, D., Kinne, S., Kleberg, D., Lasslop, G., Kornblueh, L.,
962 Marotzke, J., Matei, D., Meraner, K., Mikolajewicz, U., Modali, K., Möbis, B., Müller, W. A., Nabel, J. E.
963 M. S., Nam, C. C. W., Notz, D., Nyawira, S.-S., Paulsen, H., Peters, K., Pincus, R., Pohlmann, H.,
964 Pongratz, J., Popp, M., Raddatz, T. J., Rast, S., Redler, R., Reick, C. H., Rohrschneider, T., Schemann, V.,
965 Schmidt, H., Schnur, R., Schulzweida, U., Six, K. D., Stein, L., Stemmler, I., Stevens, B., von Storch, J.-S.,
966 Tian, F., Voigt, A., Vrese, P., Wieners, K.-H., Wilkenskjeld, S., Winkler, A., and Roeckner, E.:
967 Developments in the MPI-M Earth System Model version 1.2 (MPI-ESM1.2) and Its Response to
968 Increasing CO₂, *Journal of Advances in Modeling Earth Systems*, 11, 998–1038,
969 <https://doi.org/10.1029/2018MS001400>, 2019.

970 Menviel, L. C., Skinner, L. C., Tarasov, L., and Tzedakis, P. C.: An ice–climate oscillatory framework for
971 Dansgaard–Oeschger cycles, *Nat Rev Earth Environ*, 1, 677–693, <https://doi.org/10.1038/s43017-020-00106-y>, 2020.

973 Mylopotamitaki, D., Weiss, M., Fewlass, H., Zavala, E. I., Rougier, H., Sümer, A. P., Hajdinjak, M.,
974 Smith, G. M., Ruebens, K., Sinet-Mathiot, V., Pederzani, S., Essel, E., Harking, F. S., Xia, H., Hansen, J.,
975 Kirchner, A., Lauer, T., Stahlschmidt, M., Hein, M., Talamo, S., Wacker, L., Meller, H., Dietl, H.,
976 Orschiedt, J., Olsen, J. V., Zeberg, H., Prüfer, K., Krause, J., Meyer, M., Welker, F., McPherron, S. P.,
977 Schüler, T., and Hublin, J.-J.: Homo sapiens reached the higher latitudes of Europe by 45,000 years
978 ago, *Nature*, 1–6, <https://doi.org/10.1038/s41586-023-06923-7>, 2024.

979 Niklas, K. J.: The aerodynamics of wind pollination, *Bot. Rev*, 51, 328–386,
980 <https://doi.org/10.1007/BF02861079>, 1985.

981 Nikulina, A., MacDonald, K., Zapolska, A., Serge, M. A., Roche, D. M., Mazier, F., Davoli, M., Svenning,
982 J.-C., van Wees, D., Pearce, E. A., Fyfe, R., Roebroeks, W., and Scherjon, F.: Hunter-gatherer impact on
983 European interglacial vegetation: A modelling approach, *Quaternary Science Reviews*, 324, 108439,
984 <https://doi.org/10.1016/j.quascirev.2023.108439>, 2024.

985 Nikulina, A., Zapolska, A., Serge, M. A., Roche, D. M., Mazier, F., Davoli, M., Pearce, E. A., Svenning, J.-
986 C., Wees, D. van, Fyfe, R., MacDonald, K., Roebroeks, W., and Scherjon, F.: On the ecological impact
987 of prehistoric hunter-gatherers in Europe: Early Holocene (Mesolithic) and Last Interglacial
988 (Neanderthal) foragers compared, *PLOS ONE*, 20, e0328218,
989 <https://doi.org/10.1371/journal.pone.0328218>, 2025.

- 990 Parsons, R. W. and Prentice, I. C.: Statistical approaches to *R*-values and the pollen—vegetation
991 relationship, *Review of Palaeobotany and Palynology*, 32, 127–152, [https://doi.org/10.1016/0034-](https://doi.org/10.1016/0034-6667(81)90001-4)
992 6667(81)90001-4, 1981.
- 993 Pearce, E. A., Mazier, F., Normand, S., Fyfe, R., Andrieu, V., Bakels, C., Balwierz, Z., Bińka, K.,
994 Boreham, S., Borisova, O. K., Brostrom, A., de Beaulieu, J.-L., Gao, C., González-Sampériz, P.,
995 Granoszewski, W., Hrynowiecka, A., Kołaczek, P., Kuneš, P., Magri, D., Malkiewicz, M., Mighall, T.,
996 Milner, A. M., Möller, P., Nita, M., Noryśkiewicz, B., Pidek, I. A., Reille, M., Robertsson, A.-M.,
997 Salonen, J. S., Schläfli, P., Schokker, J., Scussolini, P., Šeirienė, V., Strahl, J., Urban, B., Winter, H., and
998 Svenning, J.-C.: Substantial light woodland and open vegetation characterized the temperate forest
999 biome before *Homo sapiens*, *Science Advances*, 9, eadi9135, <https://doi.org/10.1126/sciadv.adi9135>,
1000 2023.
- 1001 Pearce, E. A., Davison, C. W., Mazier, F., Normand, S., Fyfe, R., Serge, M.-A., Scussolini, P., and
1002 Svenning, J.-C.: Drivers of Vegetation Structure Differ Between Proposed Natural Reference
1003 Conditions for Temperate Europe, *Global Ecology and Biogeography*, 34, e70020,
1004 <https://doi.org/10.1111/geb.70020>, 2025.
- 1005 Pederzani, S., Britton, K., Jones, J. R., Pérez, L. A., Geiling, J. M., and Marín-Arroyo, A. B.: Late
1006 Pleistocene Neanderthal exploitation of stable and mosaic ecosystems in northern Iberia shown by
1007 multi-isotope evidence, *Quaternary Research*, 116, 108–132, <https://doi.org/10.1017/qua.2023.32>,
1008 2023.
- 1009 Pederzani, S., Britton, K., Trost, M., Fewlass, H., Bourgon, N., McCormack, J., Jaouen, K., Dietl, H.,
1010 Döhle, H.-J., Kirchner, A., Lauer, T., Le Corre, M., McPherron, S. P., Meller, H., Mylopotamitaki, D.,
1011 Orschiedt, J., Rougier, H., Ruebens, K., Schüller, T., Sinet-Mathiot, V., Smith, G. M., Talamo, S., Tütken,
1012 T., Welker, F., Zavala, E. I., Weiss, M., and Hublin, J.-J.: Stable isotopes show *Homo sapiens* dispersed
1013 into cold steppes ~45,000 years ago at Ilsenhöhle in Ranis, Germany, *Nat Ecol Evol*, 1–11,
1014 <https://doi.org/10.1038/s41559-023-02318-z>, 2024.
- 1015 Petit, R. J., Aguinagalde, I., de Beaulieu, J.-L., Bittkau, C., Brewer, S., Cheddadi, R., Ennos, R., Fineschi,
1016 S., Grivet, D., Lascoux, M., Mohanty, A., Müller-Starck, G., Demesure-Musch, B., Palmé, A., Martín, J.
1017 P., Rendell, S., and Vendramin, G. G.: Glacial Refugia: Hotspots But Not Melting Pots of Genetic
1018 Diversity, *Science*, 300, 1563–1565, <https://doi.org/10.1126/science.1083264>, 2003.
- 1019 Posth, C., Yu, H., Ghalichi, A., Rougier, H., Crevecoeur, I., Huang, Y., Ringbauer, H., Rohrlach, A. B.,
1020 Nägele, K., Villalba-Mouco, V., Radzeviciute, R., Ferraz, T., Stoessel, A., Tikhbatova, R., Drucker, D. G.,
1021 Lari, M., Modi, A., Vai, S., Saupe, T., Scheib, C. L., Catalano, G., Pagani, L., Talamo, S., Fewlass, H.,
1022 Klaric, L., Morala, A., Rué, M., Madelaine, S., Crépin, L., Caverne, J.-B., Bocaege, E., Ricci, S., Boschini,
1023 F., Bayle, P., Maureille, B., Le Brun-Ricalens, F., Bordes, J.-G., Oxilia, G., Bortolini, E., Bignon-Lau, O.,
1024 Debout, G., Orliac, M., Zazzo, A., Sparacello, V., Starnini, E., Sineo, L., van der Plicht, J., Pecqueur, L.,
1025 Merceron, G., Garcia, G., Leuvrey, J.-M., Garcia, C. B., Gómez-Olivencia, A., Połtowicz-Bobak, M.,
1026 Bobak, D., Le Luyer, M., Storm, P., Hoffmann, C., Kabaciński, J., Filimonova, T., Shnaider, S., Berezina,
1027 N., González-Rabanal, B., González Morales, M. R., Marín-Arroyo, A. B., López, B., Alonso-Llamazares,
1028 C., Ronchitelli, A., Polet, C., Jadin, I., Cauwe, N., Soler, J., Coromina, N., Rufí, I., Cottiaux, R., Clark, G.,
1029 Straus, L. G., Julien, M.-A., Renhart, S., Talaa, D., Benazzi, S., Romandini, M., Amkreutz, L., Bocherens,
1030 H., Wißing, C., Villotte, S., de Pablo, J. F.-L., Gómez-Puche, M., Esquembre-Bebia, M. A., Bodu, P.,
1031 Smits, L., Souffi, B., Jankauskas, R., Kozakaitė, J., Cupillard, C., Benthien, H., Wehrberger, K., Schmitz,
1032 R. W., Feine, S. C., et al.: Palaeogenomics of Upper Palaeolithic to Neolithic European hunter-
1033 gatherers, *Nature*, 615, 117–126, <https://doi.org/10.1038/s41586-023-05726-0>, 2023.

- 1034 Prentice, C., Guiot, J., Huntley, B., Jolly, D., and Cheddadi, R.: Reconstructing biomes from
1035 palaeoecological data: a general method and its application to European pollen data at 0 and 6 ka,
1036 *Climate Dynamics*, 12, 185–194, <https://doi.org/10.1007/BF00211617>, 1996.
- 1037 Prentice, I. C.: Pollen representation, source area, and basin size: Toward a unified theory of pollen
1038 analysis, *Quaternary Research*, 23, 76–86, [https://doi.org/10.1016/0033-5894\(85\)90073-0](https://doi.org/10.1016/0033-5894(85)90073-0), 1985.
- 1039 Prentice, I. C. and Harrison, S. P.: Ecosystem effects of CO₂ concentration: evidence from past
1040 climates, *Climate of the Past*, 5, 297–307, <https://doi.org/10.5194/cp-5-297-2009>, 2009.
- 1041 Pringle, R. M., Abraham, J. O., Anderson, T. M., Coverdale, T. C., Davies, A. B., Dutton, C. L., Gaylard,
1042 A., Goheen, J. R., Holdo, R. M., Hutchinson, M. C., Kimuyu, D. M., Long, R. A., Subalusky, A. L., and
1043 Veldhuis, M. P.: Impacts of large herbivores on terrestrial ecosystems, *Current Biology*, 33, R584–
1044 R610, <https://doi.org/10.1016/j.cub.2023.04.024>, 2023.
- 1045 Prüfer, K., Posth, C., Yu, H., Stoessel, A., Spyrou, M. A., Deviese, T., Mattonai, M., Ribechini, E.,
1046 Higham, T., Velemínský, P., Brůžek, J., and Krause, J.: A genome sequence from a modern human
1047 skull over 45,000 years old from Zlatý kůň in Czechia, *Nat Ecol Evol*, 5, 820–825,
1048 <https://doi.org/10.1038/s41559-021-01443-x>, 2021.
- 1049 Rasmussen, S. O., Bigler, M., Blockley, S. P., Blunier, T., Buchardt, S. L., Clausen, H. B., Cvijanovic, I.,
1050 Dahl-Jensen, D., Johnsen, S. J., Fischer, H., Gkinis, V., Guillevic, M., Hoek, W. Z., Lowe, J. J., Pedro, J.
1051 B., Popp, T., Seierstad, I. K., Steffensen, J. P., Svensson, A. M., Vallelonga, P., Vinther, B. M., Walker,
1052 M. J. C., Wheatley, J. J., and Winstrup, M.: A stratigraphic framework for abrupt climatic changes
1053 during the Last Glacial period based on three synchronized Greenland ice-core records: refining and
1054 extending the INTIMATE event stratigraphy, *Quaternary Science Reviews*, 106, 14–28,
1055 <https://doi.org/10.1016/j.quascirev.2014.09.007>, 2014.
- 1056 Reichstein, M. and Carvalhais, N.: Aspects of Forest Biomass in the Earth System: Its Role and Major
1057 Unknowns, *Surv Geophys*, 40, 693–707, <https://doi.org/10.1007/s10712-019-09551-x>, 2019.
- 1058 Reick, C. H., Raddatz, T., Brovkin, V., and Gayler, V.: Representation of natural and anthropogenic
1059 land cover change in MPI-ESM, *Journal of Advances in Modeling Earth Systems*, 5, 459–482,
1060 <https://doi.org/10.1002/jame.20022>, 2013.
- 1061 Riede, F. and Pedersen, J. B.: Late Glacial Human Dispersals in Northern Europe and Disequilibrium
1062 Dynamics, *Hum Ecol*, 46, 621–632, <https://doi.org/10.1007/s10745-017-9964-8>, 2018.
- 1063 Robin, V. and Nelle, O.: Contribution to the reconstruction of central European fire history, based on
1064 the soil charcoal analysis of study sites in northern and central Germany, *Veget Hist Archaeobot*, 23,
1065 51–65, <https://doi.org/10.1007/s00334-014-0438-2>, 2014.
- 1066 Robledo-Arnuncio, J. J.: Wind pollination over mesoscale distances: an investigation with Scots pine,
1067 *New Phytologist*, 190, 222–233, <https://doi.org/10.1111/j.1469-8137.2010.03588.x>, 2011.
- 1068 Roebroeks, W., MacDonald, K., Scherjon, F., Bakels, C., Kindler, L., Nikulina, A., Pop, E., and
1069 Gaudzinski-Windheuser, S.: Landscape modification by Last Interglacial Neanderthals, *Science*
1070 *Advances*, 7, eabj5567, <https://doi.org/10.1126/sciadv.abj5567>, 2021.
- 1071 Rogers, A. R.: Genetic Evidence for Geographic Structure within the Neanderthal Population,
1072 <https://doi.org/10.1101/2023.07.28.551046>, 24 July 2024.
- 1073 le Roux, P. C., Aalto, J., and Luoto, M.: Soil moisture’s underestimated role in climate change impact
1074 modelling in low-energy systems, *Global Change Biology*, 19, 2965–2975,
1075 <https://doi.org/10.1111/gcb.12286>, 2013.

- 1076 Rull, V.: On microrefugia and cryptic refugia, *Journal of Biogeography*, 37, 1623–1625,
1077 <https://doi.org/10.1111/j.1365-2699.2010.02340.x>, 2010.
- 1078 Saltré, F., Chadœuf, J., Higham, T., Ochocki, M., Block, S., Bunney, E., Llamas, B., and Bradshaw, C. J.
1079 A.: Environmental conditions associated with initial northern expansion of anatomically modern
1080 humans, *Nat Commun*, 15, 4364, <https://doi.org/10.1038/s41467-024-48762-8>, 2024.
- 1081 Sandel, B., Merow, C., Serra-Diaz, J. M., and Svenning, J.-C.: Disequilibrium in plant distributions:
1082 Challenges and approaches for species distribution models, *Journal of Ecology*, 113, 782–794,
1083 <https://doi.org/10.1111/1365-2745.70009>, 2025.
- 1084 Sandom, C., Faurby, S., Sandel, B., and Svenning, J.-C.: Global late Quaternary megafauna extinctions
1085 linked to humans, not climate change, *Proceedings of the Royal Society B: Biological Sciences*, 281,
1086 20133254, <https://doi.org/10.1098/rspb.2013.3254>, 2014.
- 1087 Schild, L., Ewald, P., Li, C., Hébert, R., Laepple, T., and Herzschuh, U.: LegacyVegetation: Northern
1088 Hemisphere reconstruction of past plant cover and total tree cover from pollen archives of the last
1089 14 kyr, *Earth System Science Data*, 17, 2007–2033, [https://doi.org/10.5194/essd-17-2007-](https://doi.org/10.5194/essd-17-2007-2025)
1090 2025, 2025.
- 1091 Schlüter, P.: PaleoVeg v0.1.2, , <https://doi.org/10.5281/ZENODO.15222520>, 2025.
- 1092 Schmidt, I., Hilpert, J., Kretschmer, I., Peters, R., Broich, M., Schiesberg, S., Vogels, O., Wendt, K. P.,
1093 Zimmermann, A., and Maier, A.: Approaching prehistoric demography: proxies, scales and scope of
1094 the Cologne Protocol in European contexts, *Phil. Trans. R. Soc. B*, 376, 20190714,
1095 <https://doi.org/10.1098/rstb.2019.0714>, 2021.
- 1096 Serge, M. A., Mazier, F., Fyfe, R., Gaillard, M.-J., Klein, T., Lagnoux, A., Galop, D., Githumbi, E.,
1097 Mindrescu, M., Nielsen, A. B., Trondman, A.-K., Poska, A., Sugita, S., Woodbridge, J., Abel-Schaad, D.,
1098 Åkesson, C., Alenius, T., Ammann, B., Andersen, S. T., Anderson, R. S., Andrič, M., Balakauskas, L.,
1099 Barnekow, L., Batalova, V., Bergman, J., Birks, H. J. B., Björkman, L., Bjune, A. E., Borisova, O.,
1100 Broothaerts, N., Carrion, J., Caseldine, C., Christiansen, J., Cui, Q., Currás, A., Czerwiński, S., David, R.,
1101 Davies, A. L., De Jong, R., Di Rita, F., Dietre, B., Dörfler, W., Doyen, E., Edwards, K. J., Ejarque, A.,
1102 Endtmann, E., Etienne, D., Faure, E., Feeser, I., Feurdean, A., Fischer, E., Fletcher, W., Franco-Múgica,
1103 F., Fredh, E. D., Froyd, C., Garcés-Pastor, S., García-Moreiras, I., Gauthier, E., Gil-Romera, G.,
1104 González-Sampériz, P., Grant, M. J., Grindean, R., Haas, J. N., Hannon, G., Heather, A.-J., Heikkilä, M.,
1105 Hjelle, K., Jahns, S., Jasiunas, N., Jiménez-Moreno, G., Jouffroy-Bapicot, I., Kabailienė, M., Kamerling,
1106 I. M., Kangur, M., Karpińska-Kończak, M., Kasianova, A., Kończak, P., Lagerås, P., Latalowa, M.,
1107 Lechterbeck, J., Leroyer, C., Leydet, M., Lindbladh, M., Lisitsyna, O., López-Sáez, J.-A., Lowe, J.,
1108 Luelmo-Lautenschlaeger, R., Lukanina, E., Macijauskaitė, L., Magri, D., Marguerie, D., Marquer, L.,
1109 Martinez-Cortizas, A., Mehl, I., Mesa-Fernández, J. M., Mighall, T., Miola, A., Miras, Y., Morales-
1110 Molino, C., et al.: Testing the Effect of Relative Pollen Productivity on the REVEALS Model: A
1111 Validated Reconstruction of Europe-Wide Holocene Vegetation, *Land*, 12, 986,
1112 <https://doi.org/10.3390/land12050986>, 2023.
- 1113 Shao, Y., Anhäuser, A., Ludwig, P., Schlüter, P., and Williams, E.: Statistical reconstruction of global
1114 vegetation for the last glacial maximum, *Global and Planetary Change*, 168, 67–77,
1115 <https://doi.org/10.1016/j.gloplacha.2018.06.002>, 2018.
- 1116 Shao, Y., Wegener, C., Klein, K., Schmidt, I., and Weniger, G.-C.: Reconstruction of human dispersal
1117 during Aurignacian on pan-European scale, *Nat Commun*, 15, 7406, [https://doi.org/10.1038/s41467-](https://doi.org/10.1038/s41467-024-51349-y)
1118 024-51349-y, 2024.

1119 Slimak, L., Zanolli, C., Higham, T., Frouin, M., Schwenninger, J.-L., Arnold, L. J., Demuro, M., Douka, K.,
1120 Mercier, N., Guérin, G., Valladas, H., Yvorra, P., Giraud, Y., Seguin-Orlando, A., Orlando, L., Lewis, J. E.,
1121 Muth, X., Camus, H., Vandevelde, S., Buckley, M., Mallol, C., Stringer, C., and Metz, L.: Modern
1122 human incursion into Neanderthal territories 54,000 years ago at Mandrin, France, *Science Advances*,
1123 8, eabj9496, <https://doi.org/10.1126/sciadv.abj9496>, 2022.

1124 Slimak, L., Vimala, T., Seguin-Orlando, A., Metz, L., Zanolli, C., Joannes-Boyau, R., Frouin, M., Arnold,
1125 L. J., Demuro, M., Devière, T., Comeskey, D., Buckley, M., Camus, H., Muth, X., Lewis, J. E., Bocherens,
1126 H., Yvorra, P., Tenailleau, C., Duployer, B., Coqueugniot, H., Dutour, O., Higham, T., and Sikora, M.:
1127 Long genetic and social isolation in Neanderthals before their extinction, *Cell Genomics*, 4,
1128 <https://doi.org/10.1016/j.xgen.2024.100593>, 2024.

1129 Smith, F. A., Smith, R. E. E., Lyons, S. K., and Payne, J. L.: Body size downgrading of mammals over the
1130 late Quaternary, *Science*, <https://doi.org/10.1126/science.aao5987>, 2018.

1131 Staubwasser, M., Drăgușin, V., Onac, B. P., Assonov, S., Ersek, V., Hoffmann, D. L., and Veres, D.:
1132 Impact of climate change on the transition of Neanderthals to modern humans in Europe,
1133 *Proceedings of the National Academy of Sciences*, 115, 9116–9121,
1134 <https://doi.org/10.1073/pnas.1808647115>, 2018.

1135 Stevens, R. E., Reade, H., Sayle, K. L., Tripp, J. A., Frémondeau, D., Lister, A., Barnes, I., Germonpré,
1136 M., Street, M., Murton, J. B., Bottrell, S. H., James, D. H., and Higham, T. F. G.: Major excursions in
1137 sulfur isotopes linked to permafrost change in Eurasia during the last 50,000 years, *Nat. Geosci.*, 1–5,
1138 <https://doi.org/10.1038/s41561-025-01760-x>, 2025.

1139 Strandberg, G., Brandefelt, J., Kjellström, E., and Smith, B.: High-resolution regional simulation of last
1140 glacial maximum climate in Europe, *Tellus A: Dynamic Meteorology and Oceanography*, 63, 2011.

1141 Strandberg, G., Lindström, J., Poska, A., Zhang, Q., Fyfe, R., Githumbi, E., Kjellström, E., Mazier, F.,
1142 Nielsen, A. B., Sugita, S., Trondman, A.-K., Woodbridge, J., and Gaillard, M.-J.: Mid-Holocene
1143 European climate revisited: New high-resolution regional climate model simulations using pollen-
1144 based land-cover, *Quaternary Science Reviews*, 281, 107431,
1145 <https://doi.org/10.1016/j.quascirev.2022.107431>, 2022.

1146 Sugita, S.: Theory of quantitative reconstruction of vegetation I: pollen from large sites REVEALS
1147 regional vegetation composition, *The Holocene*, 17, 229–241,
1148 <https://doi.org/10.1177/0959683607075837>, 2007.

1149 Sümer, A. P., Rougier, H., Villalba-Mouco, V., Huang, Y., Iasi, L. N. M., Essel, E., Bossoms Mesa, A.,
1150 Furtwaengler, A., Peyrégne, S., de Filippo, C., Rohrlach, A. B., Pierini, F., Mafessoni, F., Fewlass, H.,
1151 Zavala, E. I., Mylopotamitaki, D., Bianco, R. A., Schmidt, A., Zorn, J., Nickel, B., Patova, A., Posth, C.,
1152 Smith, G. M., Ruebens, K., Sinet-Mathiot, V., Stoessel, A., Dietl, H., Orschiedt, J., Kelso, J., Zeberg, H.,
1153 Bos, K. I., Welker, F., Weiss, M., McPherron, S. P., Schüler, T., Hublin, J.-J., Velemínský, P., Brůžek, J.,
1154 Peter, B. M., Meyer, M., Meller, H., Ringbauer, H., Hajdinjak, M., Prüfer, K., and Krause, J.: Earliest
1155 modern human genomes constrain timing of Neanderthal admixture, *Nature*, 638, 711–717,
1156 <https://doi.org/10.1038/s41586-024-08420-x>, 2025.

1157 Sun, Y., Xu, Q., Gaillard, M.-J., Zhang, S., Li, D., Li, M., Li, Y., Li, X., and Xiao, J.: Pollen-based
1158 reconstruction of total land-cover change over the Holocene in the temperate steppe region of
1159 China: An attempt to quantify the cover of vegetation and bare ground in the past using a novel
1160 approach, *CATENA*, 214, 106307, <https://doi.org/10.1016/j.catena.2022.106307>, 2022.

1161 Svenning, J.-C. and Sandel, B.: Disequilibrium vegetation dynamics under future climate change,
1162 *American Journal of Botany*, 100, 1266–1286, <https://doi.org/10.3732/ajb.1200469>, 2013.

1163 Svenning, J.-C., Lemoine, R. T., Bergman, J., Buitenwerf, R., Roux, E. L., Lundgren, E., Mungi, N., and
1164 Pedersen, R. Ø.: The late-Quaternary megafauna extinctions: Patterns, causes, ecological
1165 consequences and implications for ecosystem management in the Anthropocene, *Cambridge Prisms:
1166 Extinction*, 2, e5, <https://doi.org/10.1017/ext.2024.4>, 2024.

1167 Tallavaara, M., Luoto, M., Korhonen, N., Järvinen, H., and Seppä, H.: Human population dynamics in
1168 Europe over the Last Glacial Maximum, *Proc Natl Acad Sci U S A*, 112, 8232–8237,
1169 <https://doi.org/10.1073/pnas.1503784112>, 2015.

1170 Tarasov, P. E., Volkova, V. S., Webb III, T., Guiot, J., Andreev, A. A., Bezusko, L. G., Bezusko, T. V.,
1171 Bykova, G. V., Dorofeyuk, N. I., Kvavadze, E. V., Osipova, I. M., Panova, N. K., and Sevastyanov, D. V.:
1172 Last glacial maximum biomes reconstructed from pollen and plant macrofossil data from northern
1173 Eurasia, *Journal of Biogeography*, 27, 609–620, <https://doi.org/10.1046/j.1365-2699.2000.00429.x>,
1174 2000.

1175 Theuerkauf, M. and Couwenberg, J.: ROPES Reveals Past Land Cover and PPEs From Single Pollen
1176 Records, *Front. Earth Sci.*, 6, <https://doi.org/10.3389/feart.2018.00014>, 2018.

1177 Timbrell, L., Blinkhorn, J., Colucci, M., Leonardi, M., Chevalier, M., Grove, M., Scerri, E., and Manica,
1178 A.: More is not always better: downscaling climate model outputs from 30 to 5-minute resolution has
1179 minimal impact on coherence with Late Quaternary proxies, *Climate of the Past Discussions*, 1–21,
1180 <https://doi.org/10.5194/cp-2024-53>, 2024.

1181 Timmermann, A.: Quantifying the potential causes of Neanderthal extinction: Abrupt climate change
1182 versus competition and interbreeding, *Quaternary Science Reviews*, 238, 106331,
1183 <https://doi.org/10.1016/j.quascirev.2020.106331>, 2020.

1184 Timmermann, A., Yun, K.-S., Raia, P., Ruan, J., Mondanaro, A., Zeller, E., Zollikofer, C., Ponce de León,
1185 M., Lemmon, D., Willeit, M., and Ganopolski, A.: Climate effects on archaic human habitats and
1186 species successions, *Nature*, 604, 495–501, <https://doi.org/10.1038/s41586-022-04600-9>, 2022.

1187 Trepel, J., le Roux, E., Abraham, A. J., Buitenwerf, R., Kamp, J., Kristensen, J. A., Tietje, M., Lundgren,
1188 E. J., and Svenning, J.-C.: Meta-analysis shows that wild large herbivores shape ecosystem properties
1189 and promote spatial heterogeneity, *Nat Ecol Evol*, 8, 705–716, <https://doi.org/10.1038/s41559-024-02327-6>, 2024.

1191 Trondman, A.-K., Gaillard, M.-J., Mazier, F., Sugita, S., Fyfe, R., Nielsen, A. B., Twiddle, C., Barratt, P.,
1192 Birks, H. J. B., Bjune, A. E., Björkman, L., Broström, A., Caseldine, C., David, R., Dodson, J., Dörfler, W.,
1193 Fischer, E., van Geel, B., Giesecke, T., Hultberg, T., Kalnina, L., Kangur, M., van der Knaap, P., Koff, T.,
1194 Kuneš, P., Lagerås, P., Latałowa, M., Lechterbeck, J., Leroyer, C., Leydet, M., Lindbladh, M., Marquer,
1195 L., Mitchell, F. J. G., Odgaard, B. V., Peglar, S. M., Persson, T., Poska, A., Rösch, M., Seppä, H., Veski,
1196 S., and Wick, L.: Pollen-based quantitative reconstructions of Holocene regional vegetation cover
1197 (plant-functional types and land-cover types) in Europe suitable for climate modelling, *Global Change
1198 Biology*, 21, 676–697, <https://doi.org/10.1111/gcb.12737>, 2015.

1199 Tzedakis, P. C., Emerson, B. C., and Hewitt, G. M.: Cryptic or mystic? Glacial tree refugia in northern
1200 Europe, *Trends in Ecology & Evolution*, 28, 696–704, <https://doi.org/10.1016/j.tree.2013.09.001>,
1201 2013.

1202 Ukkonen, P., Aaris-Sørensen, K., Arppe, L., Clark, P. U., Daugnora, L., Lister, A. M., Lõugas, L., Seppä,
1203 H., Sommer, R. S., Stuart, A. J., Wojtal, P., and Zupinš, I.: Woolly mammoth (*Mammuthus primigenius*

- 1204 Blum.) and its environment in northern Europe during the last glaciation, *Quaternary Science*
1205 *Reviews*, 30, 693–712, <https://doi.org/10.1016/j.quascirev.2010.12.017>, 2011.
- 1206 Vancutsem, C., Achard, F., Pekel, J.-F., Vieilledent, G., Carboni, S., Simonetti, D., Gallego, J., Aragão, L.
1207 E. O. C., and Nasi, R.: Long-term (1990–2019) monitoring of forest cover changes in the humid
1208 tropics, *Science Advances*, 7, eabe1603, <https://doi.org/10.1126/sciadv.abe1603>, 2021.
- 1209 Vercauteren, N., Destouni, G., Dahlberg, C. J., and Hylander, K.: Fine-Resolved, Near-Coastal
1210 Spatiotemporal Variation of Temperature in Response to Insolation, *Journal of Applied Meteorology*
1211 *and Climatology*, 52, 1208–1220, <https://doi.org/10.1175/JAMC-D-12-0115.1>, 2013.
- 1212 Veres, D., Bazin, L., Landais, A., Toyé Mahamadou Kele, H., Lemieux-Dudon, B., Parrenin, F.,
1213 Martinerie, P., Blayo, E., Blunier, T., Capron, E., Chappellaz, J., Rasmussen, S. O., Severi, M., Svensson,
1214 A., Vinther, B., and Wolff, E. W.: The Antarctic ice core chronology (AICC2012): an optimized multi-
1215 parameter and multi-site dating approach for the last 120 thousand years, *Climate of the Past*, 9,
1216 1733–1748, <https://doi.org/10.5194/cp-9-1733-2013>, 2013.
- 1217 Vidal-Cordasco, M., Terlato, G., Ocio, D., and Marín-Arroyo, A. B.: Neanderthal coexistence with
1218 *Homo sapiens* in Europe was affected by herbivore carrying capacity, *Science Advances*, 9, eadi4099,
1219 <https://doi.org/10.1126/sciadv.adi4099>, 2023.
- 1220 Wieczorek, M. and Herzschuh, U.: Compilation of relative pollen productivity (RPP) estimates and
1221 taxonomically harmonised RPP datasets for single continents and Northern Hemisphere extratropics,
1222 *Earth System Science Data*, 12, 3515–3528, <https://doi.org/10.5194/essd-12-3515-2020>, 2020.
- 1223 Willerslev, E., Davison, J., Moora, M., Zobel, M., Coissac, E., Edwards, M. E., Lorenzen, E. D.,
1224 Vestergård, M., Gussarova, G., Haile, J., Craine, J., Gielly, L., Boessenkool, S., Epp, L. S., Pearman, P. B.,
1225 Cheddadi, R., Murray, D., Bråthen, K. A., Yoccoz, N., Binney, H., Cruaud, C., Wincker, P., Goslar, T.,
1226 Alsos, I. G., Bellemain, E., Brysting, A. K., Elven, R., Sønstebo, J. H., Murton, J., Sher, A., Rasmussen,
1227 M., Rønn, R., Mourier, T., Cooper, A., Austin, J., Möller, P., Froese, D., Zazula, G., Pompanon, F.,
1228 Rioux, D., Niderkorn, V., Tikhonov, A., Savvinov, G., Roberts, R. G., MacPhee, R. D. E., Gilbert, M. T. P.,
1229 Kjær, K. H., Orlando, L., Brochmann, C., and Taberlet, P.: Fifty thousand years of Arctic vegetation and
1230 megafaunal diet, *Nature*, 506, 47–51, <https://doi.org/10.1038/nature12921>, 2014.
- 1231 Williams, J. W. and Jackson, S. T.: Novel climates, no-analog communities, and ecological surprises,
1232 *Frontiers in Ecology and the Environment*, 5, 475–482, <https://doi.org/10.1890/070037>, 2007.
- 1233 Woillard, G. M.: Grande Pile Peat Bog: A Continuous Pollen Record for the Last 140,000 Years,
1234 *Quaternary Research*, 9, 1–21, [https://doi.org/10.1016/0033-5894\(78\)90079-0](https://doi.org/10.1016/0033-5894(78)90079-0), 1978.
- 1235 Woillez, M.-N., Kageyama, M., Krinner, G., de Noblet-Ducoudré, N., Viovy, N., and Mancip, M.:
1236 Impact of CO₂ and climate on the Last Glacial Maximum vegetation: results from the ORCHIDEE/IPSL
1237 models, *Climate of the Past*, 7, 557–577, <https://doi.org/10.5194/cp-7-557-2011>, 2011.
- 1238 Zanon, M., Davis, B. A. S., Marquer, L., Brewer, S., and Kaplan, J. O.: European Forest Cover During
1239 the Past 12,000 Years: A Palynological Reconstruction Based on Modern Analogs and Remote
1240 Sensing, *Front. Plant Sci.*, 9, <https://doi.org/10.3389/fpls.2018.00253>, 2018.
- 1241